Check for updates

Recent methods in the production of activated carbon from date palm residues for the adsorption of textile dyes: A review

Hattan A. Alharbi[1], Bassim H. Hameed[2], Khaled D. Alotaibi[3]*, Saud S. Al-Oud[3] and Abdullah S. Al-Modaihsh[3]

[1]Department of Plant Protection, College of Food and Agriculture Sciences, King Saud University, Riyadh, Saudi Arabia, [2]Department of Chemical Engineering, College of Engineering, Qatar University, Doha, Qatar, [3]Department of Soil Science, College of Food and Agriculture Sciences, King Saud University, Riyadh, Saudi Arabia

Textile dyes are organic compounds that can pose an environmental threat if not properly treated. They can cause many problems ranging from human health, ecosystem disturbances, and the reduction of the esthetic value of water bodies. The adsorption process using activated carbon (AC) has been proven to be effective in treating dyes in wastewater. However, the production of AC is limited by the non-renewables and relatively expensive precursor of coal. Date palm residues (DPRs) provide a good alternative for AC's precursor due to their continuous supply, availability in a large amount, and having good physiochemical properties such as high oxygen element and fixed carbon. This study provides a review of the potential of date palm residues (DPRs) as AC in adsorbing textile dyes and the recent technological advances adopted by researchers in producing DPR-based AC. This review article focuses solely on DPR and not on other biomass waste. This study presents a background review on date palms, textile dyes, biochar, and AC, followed by production methods of AC. In the literature, DPR was carbonized between 250 and 400°C. The conventional heating process employed an activation temperature of 576.85−900°C for physical activation and a maximum of 800°C for physicochemical activation. Chemical agents used in the chemical activation of DPR included NaOH, KOH, $ZnCl_2$, H_3PO_4, and $CaCl_2$. The maximum surface area obtained for DPR-AC was 1,092.34 and 950 m^2/g for physical and chemical activation, respectively. On the other hand, conditions used in microwave heating were between 540 and 700 W, which resulted in a surface area of 1,123 m^2/g. Hydrothermal carbonization (HTC) utilized carbonization temperatures between 150 and 250°C with pressure between 1 and 5 MPa, thus resulting in a surface area between 125.50 and 139.50 m^2/g. Isotherm and kinetic models employed in the literature are also discussed, together with the explanation of parameters accompanied by these models. The conversion of DPR into AC was noticed to be more efficient with the advancement of activation methods over the years.

1 Introduction

For the past two decades, researchers around the globe gave more attention to treating dyes in wastewater *via* adsorption processes. Due to its design flexibility, lack of treatment by-products, ease of service, high efficacy, reusability, low cost, ease of operation, and insensitivity to biological materials in aqueous settings, the adsorption approach is the most widely used remediation method (Abd El-Monaem et al., 2022; Eltaweil et al., 2022). Among all types of adsorbents, activated carbon (AC) derived from biomass and agricultural wastes has gained popularity due to two main reasons—being economically feasible and having excellent adsorption performance. One of the most utilized biomasses as an adsorbent is residues originating from date palms. Date palm (*Pheonix dactylifera* L.) is native to and widely planted in the Middle East and North African countries. Out of 120 million date palms available worldwide, 70% of them are from these countries (El-Juhany, 2010). The date palm has become the most significant fruit crop in these countries due to the overwhelming demand for date fruits around the globe. In terms of world production of date fruits, countries such as Egypt, Algeria, Iran, Saudi Arabia, Pakistan, Iraq, United Arab Emirates, Oman, Sudan, and Tunisia contribute 7,267,316 tons which is equivalent to 88.90%, followed by America and Europe with 0.58% and 0.18%, respectively (Ortiz-Uribe et al., 2019). Date fruits are graded based on several characteristics: 1) color, flavor, and sugar level, 2) moisture content, 3) physical damage on the surface, and 4) signs of insect attack. A variety of macronutrients and micronutrients can be found inside date fruits which include carbohydrates, proteins, fibers, minerals (calcium, selenium, iron, copper, magnesium, zinc, potassium, sulfur, manganese, boron, cobalt, and fluorine), and vitamin B complexes such as B1 (thiamine), B2 (riboflavin), B3 (niacin), B5 (pantothenic), B6 (pyridoxine), and B9 (folate) (Al-Harrasi et al., 2014; Eoin, 2016). This ancient tree which belongs to the Arecaceae family is also spotted to grow in other regions of the world including Mexico, Australia, South Africa, and the United States (Al-Harrasi et al., 2014; Hazzouri et al., 2015). According to Al-Alawi et al. (2017), as high as 200 genera and 2,500 species of date palms have been recorded.

Every year, it is estimated that as high as six million tonnes of date palm residues are generated (Bastidas-Oyanedel et al., 2016). These residues include date palm leaves, date palm rachis, date stones, and low quality date fruit that is not suitable to be consumed. In a year, one date palm tree has the potential to produce 2–3 kg of dried leaves which include the rachis and leaflets (Mallaki and Fatehi, 2014). Date palm leaves have no specific application but according to Chao and Krueger (2007), these residues have been traditionally utilized in house

construction, baskets, crates, and other craftwork products. El Bassam (2010) stated that 25% of the total date fruit is defined as low quality, and they make up 1.9 million tonnes of date palm residues (Al-Farsi et al., 2005). A small portion of them is being used as animal feed and in compost preparation. Date fruits are known to have a seed that is non-edible and hard in texture. This date seed is also known by other names such as date pit or date stone, and it contributes 10% of the total date weight, which translates into 0.2 million tons of date residue per year (Ahmad et al., 2011). These residues are neither suitable to be converted into fertilizers *via* composting due to low concentrations of nitrogen, nor to be incinerated due to the release of high amounts of smoke and solid into the open air (Bensidhom et al., 2018). In the literature, researchers exploit these residues and convert them into many value-added products. However, the most popular ones are AC and biochar.

It was noted that few reviews related to date palm waste utilization had been published. For instance, Tahir et al. (2020) discussed the potential of date palm waste as biochar and its applicability in different treatment processes which include adsorption process, bio-gas production, and biofuel production. Another review by Jonoobi et al. (2019) focussed on date palm waste conversion into products such as papers, adsorbents, wood composites, and fuel sources. Meanwhile, the potential of date palm waste as an adsorbent for removing heavy metals was reviewed by Shafiq et al. (2018). None of these reviews discussed the technological advancement in the production of DPR-based adsorbents and their adsorption performance in adsorbing textile dyes in depth. Henceforth, the data related to the characteristics of date palm residues (DPR), their production methods into AC, and isotherm and kinetic models to describe their adsorption behavior in removing textile dyes were reviewed in this study. This review is important to give an insight into the full potential of DPR as a good AC precursor.

2 Textile dyes

The world is facing a serious threat of water pollution due to the rapid development of economic activities and industries (Yu et al., 2019). Improper treatment of wastewater originating from these industries have caused water pollutants to enter the environment and pose a risk to living creatures (Shen, 2020). In the literature, one of the most anticipated water pollutants is textile dyes, which are consumed primarily in textile industries and other industries such as magazines, foods, leather, paper, cosmetics, and so on (Mahapatra et al., 2021). Guo et al. (2020) and Varjani et al. (2020) reported that the textile industry alone

produced 0.7 million tons of textile dyes which are lost to effluents each year, thus creating 2.15 billion tons of dye-polluted wastewater. Textile dyes are natural and synthetic compounds that can absorb radiation of light within the visible spectrum, and they are consist of two main components, chromophores and auxochromes (Barani et al., 2019; Maleki and Barani, 2019; Barani and Maleki, 2020; Haji and Naebe, 2020). Chromophores are made up of different functional groups (O=(C_6H_4) = O, -C=O, -N=N- and -NO_2) and are responsible for giving color properties to the dyes. On the other hand, auxochromes which consist of -SO_3H, -NH_3, -OH, and -COOH are known to influence the dyes' solubility through the donation or sharing of electrons (Sharma et al., 2021).

Textile dyes can be classified based on their solubility in water. Soluble dyes include acid, basic, reactive, and direct dyes whereas insoluble dyes consist of vat, sulfur, disperse, and pigment dyes (Berradi et al., 2019). Acid dyes contribute up to 30–40% of the total used dyes, and they are best to be applied to nylon and wool (Sharma and Naushad, 2020). They are also called anionic dyes since they produce negative ions upon dissociation in water. Based on the chromophore groups, acid dyes can be further divided into other major groups namely azo (acid red 27), anthraquinone (acid blue 25), and diphenylamine (acid blue 9) dyes. Chaudhary et al. (2021) reported that azo dyes are the most consumed class of dyes in the world, followed by anthraquinone dyes. Acid dyes are favored in textile industries because they bind to the fiber *via* ionic bonds, thus creating better fastness (Kert et al., 2019). Basic dyes are also known as cationic dyes due to their ability to produce positive ions as they dissociate in water. According to Yusop et al. (2021b), these ions have strong affinity toward the negative polar region of water molecules, thus making them soluble in water at a higher degree. Most of the time, basic dyes are available in the salt form of chlorides, oxalates, and zinc chloride. Sharma et al. (2021) stated that no other types of dyes can hold a candle to basic dyes when it comes to color intensity, brightness, and shades. Chemical classes of basic dyes include diphenylmethane (basic yellow 2), triarylmethane (basic green 4), azine (basic red 5), xanthene (basic violet 10), and oxazine (basic blue 12). Unlike acid dyes, reactive dyes are anionic dyes that form covalent bonds with the fiber substrate. The dyeing process usually utilizes electrolytes like NaCl and Na_2SO_4 to ease the transmission of reactive dyes to the fiber. According to Meerbergen et al. (2017), almost 70% of reactive dyes can be detected by the existence of a minimum of one azo bridge (-N=N-) in its molecular structure, and examples of these dyes are reactive red 3, reactive red 120, and reactive black 5. Direct dyes (direct blue 1, direct blue 86, and direct blue 106) are anionic dyes that can only be cold-washed since they have poor fixative properties. Although direct dyes are the cheapest type of dyes, they are extremely slow to dry up after the dyeing process due to their lack of binding properties (Sharma et al., 2021). Disperse dyes are non-ionic dyes that are conveniently vaporized to be absorbed by hydrophobic fibers.

Disperse yellow 13 and disperse violet 1 are more synonymous with dye acetates and nylon whereas disperse blue 56 and disperse blue 183 are more suitable for polyester. Vat dyes are insoluble dyes that require a reducing agent such as sodium dithionite ($Na_2S_2O_4$) to transfer the dyestuff to the fiber (Yang et al., 2021). Vat dyes such as vat blue 4 and vat green 1 provide better color fastness than reactive dyes due to the multi-ring system in their structure that enhance van der Waals forces between the dye and the substrate (Khatri et al., 2017). Sulfur dyes are organosulfur compounds and comprise a minimum of one sulfide (-S-) link in their heterocyclic rings. The world's yearly production of sulfur dyes is estimated to be 120,000 tons (Burkinshaw and Salihu, 2019). Sulfur dyes can be divided into a sulfur group (sulfur blue 15 dye) and leuco sulfur group (leuco sulfur black 1). Pigments which mean colored compounds are dominant in the printing process. Unlike other types of dyes, pigments neither have any functional groups nor a binding ability to fibers (Nguyen et al., 2016). Organic and inorganic pigments are benzoic derivatives and metal derivatives (Zn, Fe, Pb, Al, Cr, Mg, Mb, Sn, and Ca), respectively. According to Sharma et al. (2021), reactive dyes contribute the highest percentage of effluents discharged into the aquatic environment which is 10–50%, followed by sulfur dyes (10–40%), direct dyes (5–30%), acid dyes (5–20%), disperse dyes (0–10%), and lastly, basic dyes (0–5%). This type of textile dye is rarely used due to its low light fastness.

Another method to classify dyes is based on their applications. For instance, disperse dyes are dominantly applied on polyester but are sometimes also used on cellulose acetate, acrylic fibers, and nylon (Saquib and Muneer, 2003; Hassan et al., 2009). Direct dyes have a sturdy affinity toward cellulose fibers and are mostly used to color paper products (Jalandoni-Buan et al., 2010). Reactive dyes are majorly applied to cellulosic fibers and minorly applied to silk and wool fibers (Mortazavi-Derazkola et al., 2017). Vat dyes are known so far to be applied to cellulosic fibers only (Hihara et al., 2002). Basic dyes are typically applied to paper, acrylic, and nylon substrates. Some of them are also found to be used as modified polyester substrates. Acid dyes are suitable for dyeing fibers with basic functions such as polyamides (Benkhaya et al., 2020). Sulfur dyes are primarily used to dye cellulosic fibers, while azo dyes are excellent in dyeing fibers such as cotton and wool.

Many studies have been conducted on improving technologies to remove dyes from wastewater as their existence in water bodies is unwelcome due to their harmful effects. Krishna Moorthy et al. (2021) and Zarei et al. (2021) stated that dye contamination in water bodies impedes the growth of microalgae and interrupts the trophic exchange of energy and nutrients in the ecosystems. In addition to ruining the esthetic value (Yusop et al., 2021a), dyes also hinder sunlight from reaching the photic area of water bodies, thus affecting the photosynthesis process of aquatic plants (Hassan and Carr, 2018). This led to the algal bloom phenomenon, better known

as eutrophication, due to the existence of excess nitrates, nitrites, and phosphates (Rawat et al., 2018). In addition to the effect of colorization, textile dyes can also cause fluctuation in the pH level in water bodies and increase biochemical oxygen demand (BOD), chemical oxygen demand (COD), and total organic carbon (TOC) (Berradi et al., 2019). According to Khan and Malik (2018), textile dyes and the breakdown products of certain dyes like Malachite green (Zhou et al., 2019) are carcinogenic and have been linked to various diseases in plants, animals, and humans. This toxicity effect can last for a long period of time since most dyes are made up of stable aromatic compounds; thus, they are resistant to biodegradation (Dehghani et al., 2019). In a study performed by Gita et al. (2019), Drimarene blue dye was found to be highly toxic to the growth of *Chlorella vulgaris* whereas Optilan yellow and Lanasyn brown dyes demonstrated a moderate toxicity effect. A different study conducted by Krishna Moorthy et al. (2021) revealed that methylene blue dye reduced the rate of photosynthesis in *S. Platensis* and *C. Vulgaris*, thus proving the toxicity effect of this dye. Rápó et al. (2020) reported that the exposure of Eriochrome black T dye to *Eichhorniaacrassipes* and *Salvinia natans* impaired their roots and caused young leaves to develop chlorosis and necrosis. Triphenylmethane dyes such as methyl violet (MV) and brilliant green (BG) are reported to cause gastrointestinal tract and respiratory problems in humans. It was also noticed that MV has become an initiator for eye irritation whereas BG can cause skin irritation and eye redness problems (Yadav et al., 2021). A study performed by Gregoriou et al. (2020) revealed that 72.25% of the studied patients were having at least one positive reaction of allergic contact dermatitis upon exposure to hair dye allergens. Given these adverse effects caused by textile dyes, it is essential to prevent them from entering the environment by treating them effectively before discharge.

3 Biochar

Similar to AC, biochar is applied to the adsorption process to remove pollutants. Biochar is favored by some researchers over AC due to the absence of an activation step in producing it, thus reducing time, energy, cost, and materials. Since no activation process is involved, most studies show that biochar's structure is monopolized by microporosity (Chu et al., 2018; Wang et al., 2018; Zhang X. et al., 2021). Therefore, biochar is suitable to store gases such as sulfur dioxide, SO_2 (Braghiroli et al., 2019; Zhang et al., 2020), CO_2 (Huang et al., 2019; Yan et al., 2021), hydrogen sulfide, H_2S (Ma et al., 2021), and methane, CH_4 (La et al., 2019; Alimohammadi et al., 2022; Shahabi Nejad and Sheibani, 2022; Zarei et al., 2022). In terms of definition, biochar is a black carbonaceous material produced from biomass through heat treatment at temperatures higher than 250°C in the absence of air or limited air (Ben Salem et al., 2021). Because it mostly comprises carbon and contains only trace amounts of minerals

and organic matter, biochar is resistant to biodegradation and can be used as an alkaline soil amendment (Graber et al., 2010). Zama et al. (2017) stated that as biomass is dehydrated, aromatic bonds are formed from aliphatic bonds, thus resulting in stable graphene structures. Ben Salem et al. (2021), Kua et al. (2019), and Zhang et al. (2015) revealed that biochar achieved high CO_2 adsorption at certain temperatures and pressure, and these results were comparable with AC's performance.

Although most researchers found that increasing the pyrolysis temperature corresponds to biochar with better surface area for adsorption, Chaves Fernandes et al. (2020) noticed that extremely high pyrolysis temperature promotes ash formation that prevents microporous formation, thus reducing the surface area. In addition to pyrolysis temperature, the functional groups on the surface of biochar affect its adsorption capacity as well. A study conducted by Saremi et al. (2020) found that the adsorption capacity of tetracycline on date palm leaves-based biochar (DPLBC) reached 76.92 mg/g. DPLBC was subjected to surface alterations using hydrogen peroxide, cyanuric chloride, and vitamin B6 to boost the existence of carboxylic groups on its surface, thus changing the acidic properties of the surface to alkaline. Tetracycline was found to be removed 92% more completely by the altered DPLBC than it was by the original DPLBC (34%). Another work by Zubair et al. (2020a) Zubair et al. (2020a) also produced similar results, with date palm fronds-based biochar (DPFBC) adsorbing more MB dye (302.75 mg/g) after being modified with MgAl-layered hydroxide. Virgin DPFBC, in contrast, can only absorb 206.61 mg/g of MB dye.

4 Activated carbon

Date palm residues are known to be a good alternative for AC's precursor due to several advantages that they pose: 1) abundantly available and pose minimum economic value, 2) consistent supply, 3) renewables sources, 4) cheap, if not free, 5) having relatively high carbon content, and last but least, 6) existence of many functional groups inside them can enhance the adsorption process. Generally, the process of AC production can be split into two which are the carbonization process and activation process. The purpose of the carbonization process is to convert the precursor into a material that is high in carbon content (char) through a pyrolysis process at a moderate temperature between 250 and 400°C under the flow of inert gas. On the other hand, the activation process is carried out to increase pore development inside the char, thus improving the surface area. There are three types of activation processes, namely, physical, chemical, and physicochemical activation. In physical activation, the char is heated at a higher temperature than those in the carbonization process under the flow of inert gas or activating gases such as carbon dioxide, CO_2, steam, or a

combination of both. In chemical activation, the precursor does not undergo any heat treatment. Instead, activating chemical agents such as potassium hydroxide, KOH, zinc chloride, $ZnCl_2$, hydrochloric acid, HCl, sulfuric acid, H_2SO_4, and so forth are utilized to be impregnated with the char. Lastly, physicochemical activation is simply a combination of both physical and chemical activation processes. In the literature, date palm residue-based AC was found to be effective in adsorbing a variety of pollutants and posing relatively high adsorption capacity (Ogungbenro et al., 2020; Basheer et al., 2021; Haghbin and Niknam Shahrak, 2021).

Shoaib and Al-Swaidan (2015) performed physical activation on date palm tree fronds at 800 K (576.85°C) under the flow of CO_2 to produce AC (DPTFAC). DPTFAC was found to have a high surface area of 1,094 m²/g despite the relatively moderate activation temperature used. This study also revealed that a higher activation temperature than 576.85°C caused a drop in the BET surface area due to the accumulation of carbon in pores. In another physical activation study performed by Rezma et al. (2017), date palm petiole-based AC (DPPAC) was found to be dominated by microporosity with a total surface area of 546 m²/g. DPPAC was prepared under CO_2 gas flow at 900°C. One of the main reasons why researchers are more interested to activate date palm residues via chemical or physicochemical activations is because microporosity is not effective in adsorbing water pollutants as compared to mesoporosity.
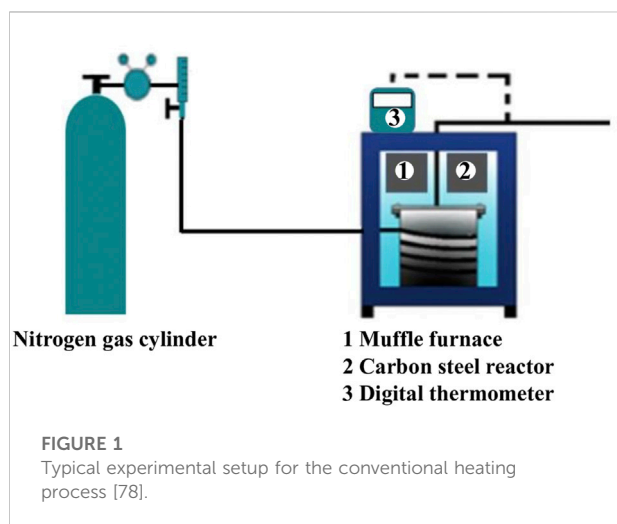
In a study performed by Melliti et al. (2021), date palm fiber was converted into AC via chemical activation using $ZnCl_2$. This AC was found to have an adsorption capacity of 147 mg/g in removing Tylosin antibiotic from an aqueous solution. In another study, sodium hydroxide, NaOH, was found to be effective in creating a mesoporous structure in date palm petiole-based AC (DPPAC), thus resulting in 53.76 mg/g adsorption capacity of indigo carmine (Khadhri et al., 2019). A similar result was found in a study carried out by Islam et al. (2015) where NaOH caused the formation of mesopore type of pores in AC prepared from palm date seeds (PDSAC), thus resulting in an adsorption capacity of 612.10 mg/g in removing methylene blue (MB) dye. This study demonstrated the importance of the impregnation ratio (IR) in affecting adsorption performance. An IR of 1:3 produced PDSAC with the highest removal percentage of MB (99.9%), followed by an IR of 1:2 and 1:1 with 88 and 56%, respectively. Another research conducted by Rambabu et al. (2021) proved that single chemical activation using KOH can produce date palm coir-based AC (DPCAC) with a high surface area of 957 m²/g, which acquired the removal of 2,4-dichlorophenoxyacetic acid by 50.25 mg/g. However, a different study showed that a low BET surface area of 143.65 m²/g was obtained when date seed-based AC

(DSAC) was calcinated with KOH at 700°C. In terms of SEM images, DSAC was observed to be mesoporous (El-Bindary et al., 2022). Rambabu et al. (2021) also found that KOH together with carbonization treatment was responsible for creating new peaks on DPCAC such as 2,355 cm⁻¹, 1459 cm⁻¹, 1269 cm⁻¹, and 601 cm⁻¹ which corresponded to hydrogen bonding, flexion of the C-H bond in CH_2 or CH_3, phenolic group and aliphatic or aromatic groups, respectively. In terms of SEM images, Kolawole et al. (2022) observed a single-layer formation of methylene blue adsorption in date pit-based AC. This AC was produced via chemical activation using H_3PO_4. Lafta et al. (2014) also used H_3PO_4 to activate the date seed, and the SEM images of this AC showed an irregular pore shape with heterogeneous morphology on its surface.

In a study performed by Haghbin and Niknam Shahrak (2021), date palm bark was subjected to physicochemical activation using phosphoric acid and heated at 400°C. The resulting AC (DPBAC) was versatile in removing many types of pollutants such as arsenic (V), methyl orange, methylene blue, and quercetin. In addition to having a high surface area of 902 m²/g, it was revealed that the adsorption of these pollutants was enhanced by the acid type of functional groups existing on DPBAC's surface. Another study performed by Daoud et al. (2017) revealed that date palm rachis-based AC (DPRAC) succeeded in removing Bezaktiv Red S-Max dye with an adsorption capacity of 128.21 mg/g. DPRAC was activated by using KOH at an activation temperature of 800°C under N_2 gas flow. KOH was found to create more basic functional groups (1.05 meq/g) than acidic functional groups (0.60 meq/g) on DPRAC's surface. Date palm fiber-based AC (DPFAC) was produced by Basheer et al. (2021) via KOH activation coupled with CO_2 gasification at 650°C. The resulting DPFAC succeeded in adsorbing 9.96 mg/g of Al^{3+}. Basheer et al. (2021) found that at a higher activation temperature, several functional groups disappeared, especially the O-H stretching vibrations, due to the inability to withstand such a high temperature. Similar to NaOH, KOH was also found to succeed in creating mesopore type of pores in DPFAC with a total surface area of 1,092.34 m²/g. Another work performed by Bouchemal et al. (2012) found that a combination of $ZnCl_2$ and CO_2 gas produced Algerian date pit-based AC (ADPAC) with a BET surface area of 1,587 m²/g. Bouchemal et al. (2012) also noticed that the SEM images of ADPAC changed from dark to a light color after the adsorption of orange G dye took place. Sait et al. (2022) conducted an SEM analysis to verify the effect of the chemical treatment of HCl and microwave radiation on the surface morphology of date seed-based AC. After the activation process took place, the surface morphology changed from a slick surface to an eroded rough surface, with a noticeable enhancement in pore size. A summary of

TABLE 1 Summary of works conducted in converting date palm residues into activated carbon.

Precursor	Activation type	Adsorbate	Adsorption capacity (mg/g)	References
Date palm tree fronds	Physical—850°C, CO_2 gas	-	-	Shoaib and Al-Swaidan, (2015)
Date palm petioles	Physical—900°C, CO_2 gas	-	-	Rezma et al. (2017)
Date palm fiber	Chemical—$ZnCl_2$	Tylosin antibiotic	147.00	Melliti et al. (2021)
Date palm petiole	Chemical—NaOH	Indigo carmine	53.76	Khadhri et al. (2019)
Date palm seed	Chemical—NaOH	Methylene blue	612.10	Islam et al. (2015)
Date palm coir	Chemical—KOH	2,4-Dichlorophenoxyacetic acid	50.25	Rambabu et al. (2021)
Date palm bark	Physicochemical—H_3PO_4, 400°C	Arsenic (V), methyl orange, methylene blue, and quercetin	0.99, 0.99, 0.98, and 0.95	Haghbin and Niknam Shahrak, (2021)
Date palm rachis	Physicochemical—KOH, 800°C, N_2 gas	Bezaktiv Red S-Max	128.21	Daoud et al. (2017)
Algerian date pits	Physicochemical—ZnCl2, 800°C, CO_2 gas	Orange G dye	-	Bouchemal et al. (2012)

Nitrogen gas cylinder

1 Muffle furnace
2 Carbon steel reactor
3 Digital thermometer

FIGURE 1
Typical experimental setup for the conventional heating process [78].

the research work conducted on converting date palm residues into AC is given in Table 1.

5 Production of activated carbon

5.1 Conventional heating

The production of activated carbon (AC) always starts with a pyrolysis process, a process that occurs in an inert atmosphere (without oxygen or a low amount of oxygen) to thermally degrade the precursor. If the precursor used is biomass, then the products that result from the pyrolysis process are biochar (solid), bio-oil (liquid), and synthesis gas (syngas). These are value-added products that can be used in various applications to support sustainability and environmentally friendly approaches.

For instance, biochar is broadly utilized as adsorbents to treat various water pollutants (Kozyatnyk et al., 2021; Luo et al., 2021; Zhu et al., 2021) and gas pollutants (Ma et al., 2021; Scheufele et al., 2021; Yuan et al., 2021). Meanwhile, bio-oil has the potential to replace hydrocarbon fuels like diesel as a transportation fuel whereas bio-syngas can be used as a heating fuel to generate electricity. The pyrolysis process is conducted using a conventional heating method which involves a conductive heat transfer mechanism from heating elements to the sample. This process takes place in a furnace or pyrolizer reactor where the energy source comes from fuel combustion or electricity. Figure 1 shows the typical experimental setup for the conventional heating process.

The first step in producing AC is called the pre-treatment or carbonization process, which is later followed by an activation process. In the carbonization process, the objective is to convert the precursor into char that is highly porous and contains a high amount of fixed carbon. The conditions applied during this process (pyrolysis temperature, pyrolysis time, and heating type) have a significant impact on the properties of the produced AC. In the literature, many researchers employed a single-stage carbonization process to produce biochar from date palm residues (DPR). For instance, Zubair et al. (2020b) carbonized date palm fronds between 500°C–800°C for 2–4 h, thus producing biochar (DPFBC) with an adsorption capacity of 206.61, 934.57, 309.59, and 280.89 mg/g in removing methylene blue, crystal violet, Eriochrome black T, and methyl orange dyes, respectively. Their study proved the versatility of date palm frond-derived biochar in removing different types of dyes. DPFBC was found to contain more surface functional groups when the carbonization temperature and time were lower and *vice versa*. A similar result was obtained by Borghol et al. (2019) where O-H, C=O, and C-O-C functional groups were found to decrease as the

carbonization temperature rose from 350 to 500°C. Another work performed by Chahinez et al. (2020) divulged that the highest removal of crystal violet dye by date palm petiole-based biochar (DPPBC) was achieved at the highest solution temperature of 40°C with an adsorption capacity of 226 mg/g. A thermodynamic study revealed that this adsorption system was governed by physisorption and behaved endothermically in nature. Chahinez et al. (2020) proposed that the micro-porosity that made up 54% of DPPBC was ultimately responsible for enhancing the adsorption of crystal violet via a pore-filling mechanism at a higher solution temperature. A similar result of the endothermic system was also observed in reactive green dye adsorption by date palm seed-based AC (Khaleefa et al., 2019) whereas the adsorption of indigo carmine by date palm petiole-based AC was found to be exothermic (Khadhri et al., 2019). In a work performed by Borghol et al. (2019), they found that by altering the surface of biochar with H_2SO_4 acid, the adsorption capacity of date palm leaf-based biochar (DPLBC) can be increased without increasing the carbonization temperature The altered DPLBC was found to adsorb methylene blue by 65.50% and 99.78% as compared to 64.80% and 96.95% for non-altered DPLBC at solution pH of 6 and 10, respectively. Surface treatment with strong acid introduced the surface of date seed biochar with acidic functional groups, namely, amine and carboxylic groups, and thus improved the affinity of ionic dyes to the surface.

The activation process on DPR is usually carried out by either physical or chemical activation alone. Some studies were observed to convert biomass into AC by using physicochemical means, but such studies that involved DPR are very limited in number. The activation step is crucial in enhancing the development of the porous network in char and increasing the surface area to a higher degree. In physical activation, the precursor is carbonized first at a moderate temperature (300°C–500°C), then followed by a gasification process using gasification agents such as water vapor, CO_2, or even air (O_2). The range of temperature used during gasification depends on the gasification agents used. If CO_2 or water vapor is used, a higher activation temperature (700°C–900°C) is selected. However, if air is used, a lower temperature (300°C–450°C) is utilized due to the higher reactivity level of O_2 than water vapor and CO_2 (Lewoyehu, 2021). In the literature, the majority of publications from 2016 until now were noticed to utilize chemical activation to activate DPR. In addition to requiring a lower activation temperature, chemical activation is favored by researchers due to the better porosity that it can give to the sample than physical activation. Furthermore, the yield of carbon and the surface area are higher in chemical activation than those in physical activation, due to dehydrogenation properties of the chemical agents that retard tar formation and lessen volatile products (Lewoyehu, 2021). Like physical activation, chemical activation also starts with char production via a pyrolysis process. The char is then impregnated with dehydrating agents at a

certain impregnation ratio (IR) for a certain activation period. After that, the impregnated char is washed to remove excess chemical agents from blocking the pores on the sample. However, in two-stage chemical activation, the impregnated char is subjected to another heat treatment before the washing process. Common chemicals used to impregnate DPR are metal salts, namely, potassium hydroxide (KOH), zinc chloride ($ZnCl_2$), phosphoric acid (H_3PO_4), calcium chloride ($CaCl_2$), sodium hydroxide (NaOH), and others. During the impregnation process, metallic atoms penetrate deep inside the char's structure via intercalation, henceforth creating new pores and expanding the size of existing pores (Villota et al., 2019; Ge et al., 2020).

Selection of the right chemical agents is important to activate the different types of precursors used. Mustafa and Asmatulu (2020) compared the characteristics between $ZnCl_2$-activated date seed (Zn-ADS) and $CaCl_2$-activated date seed (Ca-ADS). N_2 adsorption isotherm in Zn-ADS and Ca-ADS was found to follow type I and type II, respectively, which signified that $CaCl_2$ promoted microporosity better than $ZnCl_2$. The BET surface area of Zn-ADS and Ca-ADS was 591.43 and 76.94 m^2/g, respectively, thus validating the effectiveness of $ZnCl_2$ as a chemical agent compared to $CaCl_2$. In a study conducted by Daoud et al. (2017), KOH was found to be effective in creating a high microporous surface area (837 m^2/g) in date rachis-based AC. Jabbar (2020) compared the role of different chemicals such as $ZnCl_2$, KOH, and H_2SO_4 in activating date stones (DSAC) to remove methyl orange and bismark brown dyes. It was revealed that KOH produced DSAC with the highest surface area (950 m^2/g), followed by H_3PO_4 (815 m^2/g) and $ZnCl_2$ (600 m^2/g), thus proving the superiority of KOH as the better chemical agent. Unfortunately, these surface areas were dominated by micro-porosity, henceforth producing low adsorption capacity between 0.96–1.74 mg/g for methyl orange and 0.51–0.90 mg/g for bismark brown. The domination of micro-porosity in these ACs was contributed by the usage of N_2 as an activating agent, which is less effective in widening the pores on ACs than CO_2 and steam. On the contrary, NaOH was found to be responsible in creating mesoporosity in date palm petiole-based AC (DPPAC), which is favorable to adsorb 53.76 mg/g of indigo carmine dye in an aqueous solution (Khadhri et al., 2019). The adsorption of indigo carmine into DPPAC was found to be contributed by physisorption which involved a weak electrostatic attraction and hydrogen bonding between carboxylic, phenolic, and lactonic functional groups with C=O, N-H, and SO_3 from indigo carmine's structure. Daoud et al. (2017) revealed that under the same chemical activation condition using KOH (IR of 0.74), the type of pores existing on date palm rachis-based AC (DPRAC) and jujube stone-based AC (JSAC) was different. The N_2 adsorption–desorption isotherm showed that JSAC followed type I which signified the dominance of micropores. On the contrary, the curve for DPRAC exhibited type I and type II, therefore confirming the combination of micropores and

TABLE 2 Summary of the literatures on converting date palm residues into activated carbon *via* conventional heating.

Precursor	Summary of the method	Yield (%)	Surface area (m²/g)	Dyes	Adsorption capacity (mg/g)	References
Date stones	Carbonization at 275°C for 90 min, then soaked in H_3PO_4 or KOH or $ZnCl_2$ for 24 h, followed by activation at 600°C using N_2 gas for 2 h	-	815 (date + H_3PO_4)	Methyl orange (MO) and bismark brown (BB)	1.74 (MO-date + H_3PO_4)	Jabbar, (2020)
					0.96 (MO-date + KOH)	
			950 (date + KOH)		1.61 (MO-date + $ZnCl_2$)	
					0.90 (BB-date + H_3PO_4)	
			600 (date + $ZnCl_2$)		0.55 (BB-date + KOH)	
					0.51 (BB-date + $ZnCl_2$)	
Date palm petiole	Carbonization at 600°C for 2 h, followed by chemical activation with NaOH at IR of 2 for 12 h, then carbonized again at 600°C for 2 h	-	655.00	Indigo carmine	53.76	Khadhri et al. (2019)
Date pits	Impregnation with H_2SO_4 for 24 h, followed by carbonization at 400°C under N_2 gas for 2 h	-	-	Methylene blue, methyl orange, congo red and eosin yellowish	91.91%, 90.23%, 64.29%, and 56.11%	Mohammed et al. (2018)
Date seeds	Carbonization at 243°C for several minutes using N_2 gas	-	-	Methylene blue	30.03	El Marouani et al. (2018)
Date palm rachis	Impregnation with KOH at IR of 0.74, followed by carbonization at 800°C for 1 h	-	1160.00	Bezaktiv Red S-Max	128.21	Daoud et al. (2017)
Date palm bark	Impregnation with 85% H_3PO_4 at IR of 0.4 for 24 h, followed by carbonization at 400°C for 3 h	52.00	902.00	Methylene blue, methyl orange, and quercetin dyes	99.96%, 99.91%, and 97.62%	Haghbin and Niknam Shahrak, (2021)
Date palm fronds	Carbonization at 700°C for 4 h, followed by surface modification using MgAl salts	-	443.39	Methylene blue	302.75	Zubair et al. (2020a)
Date palm fronds	Carbonization at 500–800°C for 2–4 h	12.22–29.54	431.82	Methylene blue, crystal violet, Eriochrome black T, and methyl orange	206.61, 934.57, 309.59, and 280.89	Zubair et al. (2020b)
Date palm leaf	Carbonization at 800°C for 180 min	-	-	Methylene blue	359.64	Shafiq et al. (2019)
Date palm petioles	Carbonization at 700°C for 3 h	-	640.00	Crystal violet	209.00	Chahinez et al. (2020)
Date palm leaf	Carbonization at 450°C for 2 h, then followed by chemical activation using sulfuric acid at 40–50°C	31.00	-	Methylene blue	96.60%	Borghol et al. (2019)
Date seeds	Carbonization at 350C for 5 h, followed by chemical activation using 98 wt% sulfuric acid at room temperature for 1 h	-	-	Reactive green	8.06	Khaleefa et al. (2019)
Date stones	Impregnation with H2SO4, followed by carbonization for 8 h	-	-	Methylene blue and crystal violet	515.46 and 543.47	Messaoudi et al. (2016)

mesopores. Due to this, the adsorption capacity of DPRAC in removing Bezaktiv Red S-Max dye was 128.21 mg/g which is way superior than the adsorption capacity obtained for JSAC which is 28.49 mg/g. Rambabu et al. (2021) explored the reversed single-stage chemical activation method where the raw date coir was impregnated with KOH first before being carbonized at 650°C, which resulted in a moderately high surface area of 947 m²/g. This route of activation generated a wide range of O-bearing surface groups in date coir-based AC. A similar method was employed by Mumtaz et al. (2021) where raw date stones were

impregnated with 85% H_3PO_4 before undergoing carbonization at 800°C for 45 min. This reversed method was noted to be beneficial in removing excess chemical agents *via* evaporation. However, according to Lewoyehu (2021), this reversed one-stage chemical activation is not suitable if KOH or NaOH is used since these strong bases can dissolve the organic matter in PDR, making it impractical for the subsequent activation process to be carried out.

Typical physicochemical activation starts with a carbonization process, followed by chemical activation and

ending with physical activation. This hybrid type of activation is usually noticed to produce a higher surface area in AC than physical and chemical activations alone. Theoretically, during chemical activation, the metallic ions penetrate deep into the skeleton of the char's matrix and creating a porous network, mostly in micropore size. Then, the following physical activation process caused the molecules of activating gases to diffuse inside the micropore type of pores and bombarde them vigorously, therefore enhancing the size of the pores from micropores to mesopores, and in some cases, to macropores. Therefore, researchers choose physicochemical activation because the resultant AC is suitable to adsorb water pollutants such as dyes, heavy metals, pharmaceutical residues, and so on, due to their relatively larger molecule size than that of gas pollutants. However, the requirement for an extra step, the need to use both chemical agents and activating gases, thus increasing the total cost production of AC, had demotivated researchers from taking this route to activate DPR. Nonetheless, an optimization study conducted by Basheer et al. (2021) revealed that date fiber-based AC (DFAC) with a high surface area of 1,092.34 m^2/g was successfully produced with KOH activation coupled with CO_2 gasification. Unfortunately, CO_2 gasification caused several functional groups (C-O stretching vibration in ester, ether, or phenol) to become less intense in DFAC. A similar result where gasification weakened the intensity of functional groups in DPR-based AC was obtained in a work performed by O. Basheer et al. (2019). Table 2 summarizes the works on converting DPR into AC *via* conventional heating.

5.2 Microwave heating

These days, microwave heating (MH) has become the preferred technique in carbonizing and/or activating the precursor in AC production. Although the fundamental of the MH process is still a lot to unfold and understand, results from many studies have shown that this heating technique is far superior to conventional heating (CH), in many aspects. Technically, microwave belongs in the spectrum of electromagnetic with a wavelength range between 1 mm and 1 m, and microwave energy can be defined as non-ionizing electromagnetic radiation with frequencies that operate at three different bands. These bands are ultra-high frequency, super high frequency, and extremely high frequency which correspond to 300 MHz–3 GHz, 3 GHz–30 GHz, and 30 GHz–300 GHz, respectively (Haque, 1999). The frequency of microwaves utilized in medical, industrial, and domestic sectors are tuned to operate at a value between 915 and 2,450 MHz. At these frequencies, the conversion rate from electrical energy to microwave energy is 85% and 50%, respectively (Huang et al., 2016). The heating principle in MW is completely different from the one in CH. In CH, heat is transmitted from the outer surface of the matter to solid bulk

via a conduction process, henceforth producing an uneven heating gradient (Hoseinzadeh Hesas et al., 2012; Motasemi and Afzal, 2013). On the contrary, MW is accomplished by the induced rotation of valence electrons at an extremely high speed by electromagnetic waves, thus converting the kinetic energy of electrons (rotational, vibrational, and translational motion) into heat dissipation that heats the whole matter (Rossi et al., 2017). Since MH is driven by induced polarity, the transformation of electromagnetic into thermal energy occurs at uniform and volumetric states, which signifies a faster heating process than CH (Omoriyekomwan et al., 2021). MH is known for its ability to heat different materials at different rates (selective heating) based on the nature of the interaction between microwave energy and the material's properties. Based on this selective heating principle, materials can be distinguished into three types: 1) microwave dielectrics (absorber) which absorb and convert microwave energy into the dissipation of heat such as water and oils, 2) microwave-transparent materials (insulators) which permit microwave energy to pass through them without absorbing any such as Teflon and quartz, and 3) microwave conductors which reflect microwave energy such as metals (Li et al., 2020).

The effectiveness of microwave energy in heating a matter depends mainly on the dielectric properties of the matter itself, which can be evaluated by the dielectric loss tangent. According to Zlotorzynski (1995), the dielectric loss tangent is a ratio of the dielectric constant (the matter's potential in reflecting microwave energy) to dielectric loss factor (the matter's potential in absorbing microwave energy, which corresponds directly to the amount of heat dissipated by microwave energy). The value of the dielectric loss tangent for commercial ACs and coal was determined to be 0.22–2.95 and <0.10, respectively (Marland et al., 2001; Dawson et al., 2008). The temperature of the sample in the MH technique is not suitable to be measured using a metallic thermocouple since microwave radiation causes an independent heating process of the sample under the Joule effect (Sasi Kumar et al., 2020). In other words, the temperature measurement made by the thermocouple is not accurate since it only measures the external surface of the sample whereas the internal local heating effects are neglected. Therefore, many studies were observed to use radiation power instead (Ahmad et al., 2021; Yusop et al., 2022a; Yusop et al., 2022b; Mohamad et al., 2022). Figure 2 shows the comparison between microwave and conventional heating methods.

The switch from CH to MH by researchers is driven by many factors and one of them is the environmental impact. Depending on the nature of the precursor and the process conditions employed, it was estimated that the production of 1 ton of AC *via* CH can consume 170–200 kWh of electrical energy which corresponds to 127.50–150.00 kg CO_2 released per 1 ton of AC. This is similar to the effect of burning 160–188 kg of coal (Sasi Kumar et al., 2020). On the contrary, the amount of electrical energy used in MH can be reduced

FIGURE 2
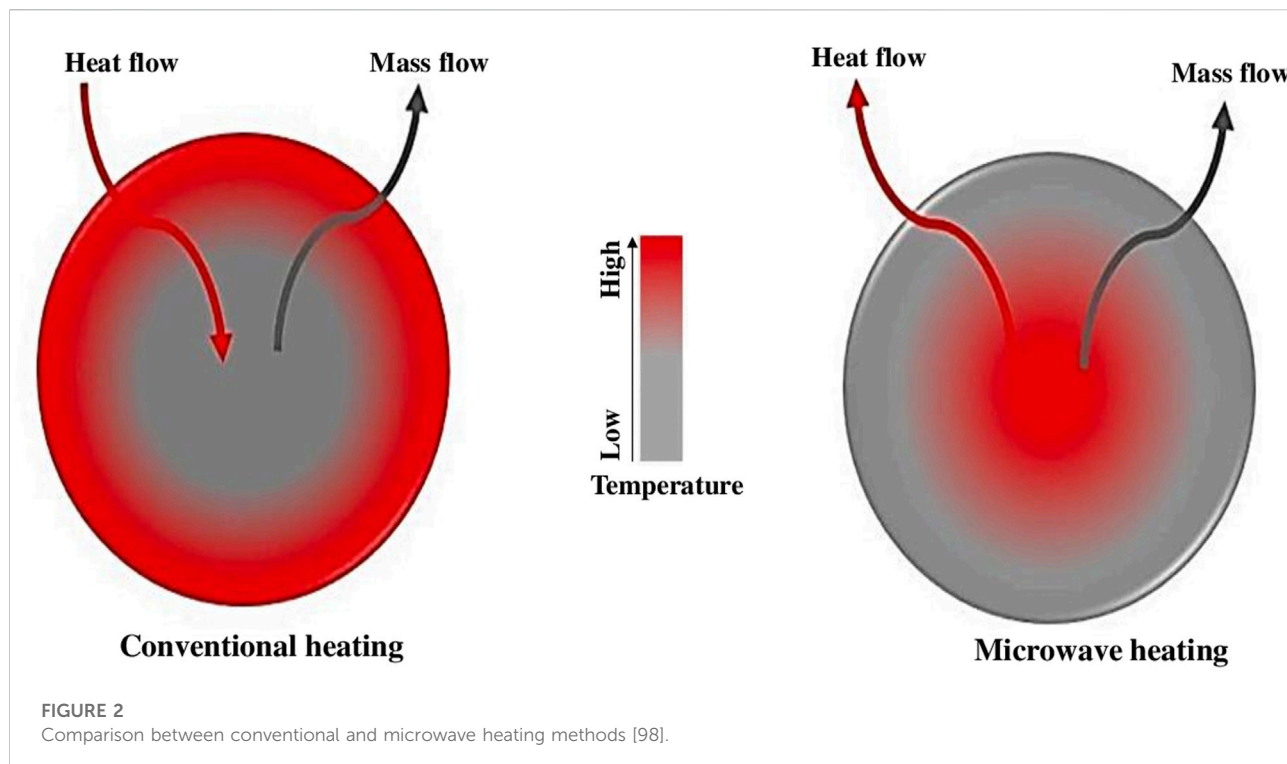Comparison between conventional and microwave heating methods [98].

TABLE 3 Differences between CH and MH (Li et al., 2018; Liang et al., 2019; Haeldermans et al., 2020; Sasi Kumar et al., 2020; Mohamed et al., 2021; Mari Selvam and Paramasivan, 2022).

Conventional heating	Microwave heating
Heating process occurs *via* conduction and conventional heat transfer	Heating process occurs *via* radiation heat transfer
Sample is heated from the external surface to the inward surface	Sample is heated from the internal surface to the outward surface
Required longer activation time (2–22 h)	Required shorter activation time (10–15 min)
Total cost for activation gas and electricity are higher due to longer activation time	Total cost for activation gas and electricity are lower due to shorter activation time
Temperature of the sample can be measured using a metallic thermocouple	Due to the nature of independent heating of the process under the Joule effect, temperature of the sample cannot be determined accurately, therefore, radiation power is used instead
Required a decrease in sample size before activation to increase surface area to mass ratio	No requirement to decrease the sample size before activation to increase the surface area to mass ratio
Produce AC with relatively lower yield	Produce AC with relatively higher yield
Non-instantaneous reaction	Instantaneous reaction
Non-selective heating	Selective heating
Polarity of the sample has no effect on heating process	Polarity of the sample uniquely affects the microwave heating

significantly due to an extremely shorter period of time required to carbonize and/or activate the sample (10–15 min) compared to CH (2–22 h) (Li et al., 2018). More differences between CH and MH are summarized in Table 3.

Throughout the literature, several studies exploited MH in producing AC from DPR, although the number of such publications is much lower than the ones that use CH. In a study conducted by Hijab et al. (2021), a comparison was made between CH and MH in producing date stone-based AC (DSAC). It was found that microwave heated-DSAC achieved a significantly higher BET surface area and total pore volume of 1123 m^2/g and 0.72 cm^3/g, respectively, than conventional heated-DSAC with 669 m^2/g and 0.46 cm^3/g, respectively. Microwave-heated DSAC was also noticed to have a higher adsorption capacity of 98 mg/g in removing malachite green dye than conventional heated-DSAC with 58 mg/g. A similar

TABLE 4 Summary of works conducted in converting date palm residues into activated carbons *via* microwave heating.

Precursor	Summary of method	Yield (%)	Surface area (m²/g)	Dyes	Adsorption capacity (mg/g)	References
Date stone	Chemical activation with 30% H_3PO_4 at IR of 1, followed by microwave heating at 850 W for 7 min	-	1123.00	Malachite green	98.00	Hijab et al. (2021)
Date stone	Chemical activation with 80% H_3PO_4 at IR of 2, followed by microwave heating at 900 W for 7 min	-	1123.00	Malachite green	95.25	Hijab et al. (2020)
Date stone	Chemical activation with K_2CO_3 at IR of 1.5 for 24 h, followed by microwave heating at 660 W for 8 min	19.99	1144.25	Methylene blue	460.12	Abbas and Ahmed, (2016)
Date spathe	Chemical activation with 40% H_3PO_4 at IR of 3 for 24 h, followed by microwave heating at 700 W at 2 min	54.00	794.70	Methyl orange	224.40	Emami and Azizian, (2014)
Date stone	Carbonization at 700 °C, followed by chemical activation with KOH at IR of 1.75, then microwave heating at 600 W for 8 min	-	856.00	Methylene blue	316.11	Foo and Hameed, (2011)

result was obtained in a different study by Hijab et al. (2020) where the removal of malachite green dye was more effective using microwaved-treated DSAC (95.25 mg/g) than the conventional-heated DSAC (58.10 mg/g). An optimization study of converting date stones into AC (DSAC) *via* K_2CO_3 chemical activation and the MH technique was conducted by Abbas and Ahmed (2016). Their study concluded that a relatively low radiation time of 8 min and a relatively moderate IR of 1.50 were successful in producing DSAC with optimum adsorption uptakes of 460.12 mg/g in removing methylene blue and an optimum yield of 19.99%. This study also revealed that by increasing radiation power, radiation time, and IR beyond 660 W, 8 min, and 1.50, respectively, both adsorption capacity and IR decreased. The reduction in adsorption capacity was driven by the conversion of mesopores into macropores which is not suitable to adsorb methylene blue whereas the drop in yield was contributed by the formation of an unstable structure of DSAC at such extreme conditions. In terms of functional groups, several new ones were found to be formed, especially O-H groups (alcohol, phenol, and carboxylic acid), which was in agreement with the results obtained by Khan T. M. et al. (2019).

In a different study by Abbas et al. (2016) that utilized the same DPR of date stones and the same activation method (K_2CO_3 chemical activation coupled with MH), a much higher yield of 44% was achieved due to the lower radiation power used, 540 W, as compared to 19.99% (660 W) in the study performed by Abbas and Ahmed (2016). Their study stated that the MH technique had reduced the degree of burn-off significantly as compared to CH, and thus, a higher yield can be obtained. Emami and Azizian (2014) also reported the ability of MH in producing a high yield of 54% in the production of date spathe-based AC (DSPAC), despite using high radiation power and IR of 700 W and 3, respectively. This study proved that high yield can be achieved at such extreme conditions as long as the radiation time is low enough, which in this case, is 2 min. It was a noteworthy observation that when the radiation time was prolonged to 5 min and above, the bonds of C-O-C and C-C were

broken and the carbon structures were burned off, henceforth reducing the surface area and adsorption uptakes. MH was also responsible for creating mesoporosity in DSPAC, as confirmed by the hysteresis loop obtained in the N_2 adsorption–desorption isotherm, thus explaining the good adsorption capacity of 224.40 mg/g in adsorbing methyl violet dye. The first work that employed MH in converting DPR into AC was conducted by Foo and Hameed (2011). In their study, the date stone was impregnated with KOH at an IR of 1.75, followed by MH at 600 W and 8 min for radiation power and radiation time, respectively. The resultant AC was found to have a relatively high surface area (1275 m²/g) and adsorption capacity (316.11 mg/g) for methylene blue dye adsorption, thus validating the results from later studies where relatively moderate activation conditions can produce DPR-based AC with good properties. Their study also obtained similar results as Emami and Azizian (2014) where the N_2 adsorption–desorption isotherm followed type I and II, which signified the existence of micropores and mesopores. Table 4 summarizes the work conducted on converting DPR to AC *via* the MH technique.

5.3 Hydrothermal carbonization (HTC) process

In addition to the pyrolysis process, the carbonization step in AC production can be carried out using the hydrothermal carbonization (HTC) process. The resultant char from the pyrolysis process is called "pyrochar" whereas the one that is produced from the HTC method is commonly referred to as "hydrochar." Table 5 shows the summary of the comparison between pyrolysis and HTC processes. Basically, HTC is a thermo-chemical process that converts feedstock into carbon-rich hydrochar and this process behaves exothermically where the reduction of oxygen and hydrogen components in the feedstock occurs mainly *via* dehydration and decarboxylation (Funke and Ziegler, 2010). Together with HTC, hydrothermal liquefaction (HTL) and hydrothermal gasification (HTG) are two sub-categories under hydrothermal heat treatment where their differences rely on

TABLE 5 Summary of the comparison between pyrolysis and hydrothermal carbonization (Khan T. A. et al., 2019).

	Pyrolysis process	Hydrothermal carbonization
Main reaction	Combustion	Dehydration
Input	Dry	Wet
Temperature	400–900°C	180–350°C
Reaction	$C_6H_{10}O_5$ (s) $\Delta \rightarrow$ 6C (s) + $5H_2O$ (l)	$C_6H_{10}O_5$ (s) + H_2O (l) $\Delta \rightarrow C_6H_2O$ (s) + $5H_2O$ (l)
Process agent	None	Water
Primary product	Oil	Char
By-product	Char	Volatile liquid + CO_2

the process conditions applied. For instance, HTC is carried out at a temperature between 150 and 250°C and pressure between 1 and 5 MPa whereas HTL and HTG are performed at much higher temperatures (>300°C and >380°C) and higher pressure (>12 MPa and >22 MPa), respectively (Kruse, 2008). Generally, the main products from the hydrothermal process are solid products (hydrochar), liquid products (bio-oil), and gas products (syngas such as CH_4, CO, and CO_2) where the properties of these products significantly depend on the type of the feedstock and the process conditions utilized (Sun et al., 2014).

HTC provides a better option to carbonize biomass due to several key advantages that it offers which include: 1) lower temperature condition (180–350°C), 2) an effective carbonization technique for wet biomass with the exclusion of energy consumption for the drying step (Benavente et al., 2015), 3) the agent used (water) is environmentally friendly, non-toxic, and inexpensive (Knez et al., 2015), 4) practical to be implemented, and 5) large-scale applicability (Okajima and Sako, 2013). According to Khan T. A. et al. (2019), hydrochar demonstrates brittle and extreme hydrophobic properties, thus causing its separation from the liquid solution to be hassle-free. Similar to AC, the hydrochar is versatile in adsorbing a variety of contaminants such as heavy metals (Li S.-Y. et al., 2021; Zhang et al., 2022), dyes (Li H.-Z. et al., 2021; Lv et al., 2022), gases (Sultana et al., 2021), antibiotics (Qu et al., 2021), phenolic compounds (Marx et al., 2021; Pauletto et al., 2021), and so forth. In addition to being utilized in adsorption processes as an adsorbent, hydrochar is also used in other applications such as promoting anaerobic digestion in activated sludge (He et al., 2021; Shi et al., 2021), composite material applications (Nizamuddin et al., 2021), hydrogen gas production (Lin et al., 2021), biofuel applications (Zhang Z. et al., 2021), chemical sensing applications (Espro et al., 2021), and others.

Unlike the pyrolysis process that is carried out in a dry condition, HTC is accomplished by adding supercritical water to the feedstock. A study conducted by Olszewski et al. (2020) confirmed that the pyrolysis process coupled with HTC

improved the surface area of the precursor (spent grains) to 139.50 m^2/g as compared to the one that underwent pyrolysis alone (82 m^2/g). In addition, char yield, carbon content, and porosity were noticed to increase whereas ash content was seen to decrease. It was concluded by Behar et al. (2003) that the quantity of supercritical water used in the HTC process majorly influenced the composition distribution of the products. Supercritical water is known to have a temperature of 300°C, density of 713 kg/m^3, dielectric constant of 19, ionization constant of 10^{11}, and is miscible in organic compounds. Due to this, the potential for bonds such as OH and COOH in lignocellulosic materials to break down and become miscible with the supercritical water is exceptionally high. In addition, other prominent functions of supercritical water during the HTC process include 1) becoming a mobile intermediate for ions which participate from one bond to another, 2) causing inactive bonds to break down and connect them back with different compounds in an arbitrary order, and 3) causing a rapid hydrolysis process on lignocellulosic materials that is driven by *in situ* acid and/or base catalyzation due to a high ionization constant which reflects the excess number of H^+ and OH^- at a subcritical state (Kruse, 2008; Khan T. A. et al., 2019).

In the literature, only few publications have employed the HTC method to convert DPR into hydrochar. In a study performed by El Ouadrhiri et al. (2021), optimum preparation conditions for date seed-based hydrochar (OHC-DS) were found to be 200°C, 120 min, and 20 mg of temperature, reaction time, and catalyst dose (citric acid), respectively, which corresponded to hydrochar yield of 59.71% and 75.84% of the carbon retention rate. It was observed that when the temperature and residence time were increased from 160 to 240°C and from 32 to 120 min, respectively, the yield of OHC-DS decreased accordingly. A similar result was also obtained by using different types of lignocellulosic materials as conducted by Kristianto et al. (2020). Such results were driven by the fact that at a higher temperature and residence time, HTC promotes dehydration, condensation, aromatization, and polymerization processes to occur at a higher degree (Sevilla and Fuertes, 2009; Hu et al.,

TABLE 6 Summary of works conducted for converting date palm residues into hydrochar *via* the hydrothermal carbonization process.

Precursor	Summary of the method	Yield (%)	Surface area (m^2/g)	Adsorbate	Adsorption capacity (mg/g)	References
Date seed	HTC was carried out in a polypropylene-lined autoclave with a biomass to water ratio of 1:10. 20 mg of citric acid as a catalyst was added to the mixture, then stirred well. Temperature and residence time used were 200°C and 120 min, respectively. Hydrochar was further activated using KOH and pyrolyzed at 600°C	59.71	1251.50	Methylene blue and methyl orange	657.89 and 384.61	El Ouadrhiri et al. (2021)
Date seed	5 g of date seed together with 100 ml of water was heated at 200°C for 5 h. Hydrochar was further activated using NaOH at IR of 3 and pyrolyzed at 600°C	-	1282.49	Methylene blue	612.10	Islam et al. (2015)

2010). El Ouadrhiri et al. (2021) also concluded that the production of hydrochar *via* acid citric-catalyzed HTC was dominated by dehydration and decarboxylation whereas at a temperature between 200 and 233°C, the main reaction that occurred was demethanization. Further alteration of OHC-DS with KOH treatment and pyrolysis process at 600°C produced an active material (AOHC-DS) with a high surface area of 1251.50 m^2/g and high adsorption capacity of 657.89 and 384.61 mg/g for methylene blue and methyl orange dyes, respectively. Henceforth, this study proved that HTC is an effective carbonization route for preparing AC.

Islam et al. (2015) produced date palm seed-based AC (PDSAC) *via* HTC and NaOH chemical activation. The resultant PDSAC was dominated by mesopore type of pores, a relatively high surface area of 1282.49 m^2/g, and high adsorption capacity of 612.10 mg/g in adsorbing methylene blue. It was revealed that HTC caused the porosity development in hydrochar to be less impactful due to recondensation of volatile matter. Nonetheless, HTC was found to affect the hemicellulose, cellulose, and lignin compounds of the precursor's cell wall, thus altering the properties of the hydrochar's surface. This alteration aided the transfer of NaOH into the hydrochar's structure. FTIR analysis confirmed that the HTC process was responsible for removing the peaks at 806 and 756 cm^{-1} (C-O of mono-substituted benzene ring) whereas the peak at 1014 cm^{-1} (C-O stretch in cellulose and hemicellulose) shifted to 1,026 cm^{-1}. The role of supercritical water in breaking down and connecting bonds was verified by the formation of new peaks after HTC treatment such as 2,924 cm^{-1} (C-H stretching of alkanes), 1,705 cm^{-1} (C=O stretching of aliphatic ketone), 1,608 cm^{-1} (C=C stretching of conjugated alkene), 1,508 cm^{-1} (N-O asymmetric stretching of the nitro compound), 1,435 cm^{-1} (O-H bending of carboxylic acids), 1,280 cm^{-1} (C-O stretching of esters), 1,234 cm^{-1} (S=O stretching of sulfonate), 1,207 cm^{-1} (C-O stretching of esters), 1,161 cm^{-1} (S=O stretching of sulfonate), 1,111 cm^{-1} (C-O stretching of aliphatic ether), and 1,056 cm^{-1} (C-O

stretching of alcohol). Table 6 shows the summary of works conducted in converting DPR into hydrochar *via* HTC.

6 Adsorption of textile dyes on date palm-derived activated carbons

6.1 Adsorption isotherms

The adsorption process involves the accumulation of adsorbate molecules (liquid or gas phase) on the surface of a porous solid material known as the adsorbent. When an adsorbent is introduced into a system that is filled with adsorbate molecules, a portion of the adsorbate molecules find their way to enter the pores that exist on the adsorbent and eventually, those adsorbate molecules are adsorbed to the surface of the adsorbent *via* physisorption or chemisorption (Sims et al., 2019). Figure 3 shows the mass transfer steps during the adsorption process.

Physisorption is contributed by electrostatic interaction (dipole–dipole forces, London forces, and van der Waals) that is weak and can be ruptured rather easily as compared to chemisorption that is formed *via* strong covalent bonds through the electron sharing or transferring. Physisorption is known to cause multilayer coverage and involves reversible processes whereas chemisorption corresponds to monolayer coverage and irreversible processes. The adsorbed adsorbate molecules are known as "adsorbates in the solid phase" whereas the remaining adsorbate molecules that are not adsorbed by the adsorbent are called "adsorbates in the bulk phase."

Throughout the adsorption process (from the beginning until adsorption equilibria are attained), the concentration of the adsorbate molecules in both solid and bulk phases form a dynamic relationship that can be understood *via* the application of an isotherm model. In addition, according to Yamil et al. (2021), an isotherm study is vital in determining the maximum adsorption capacity of certain adsorbate molecules
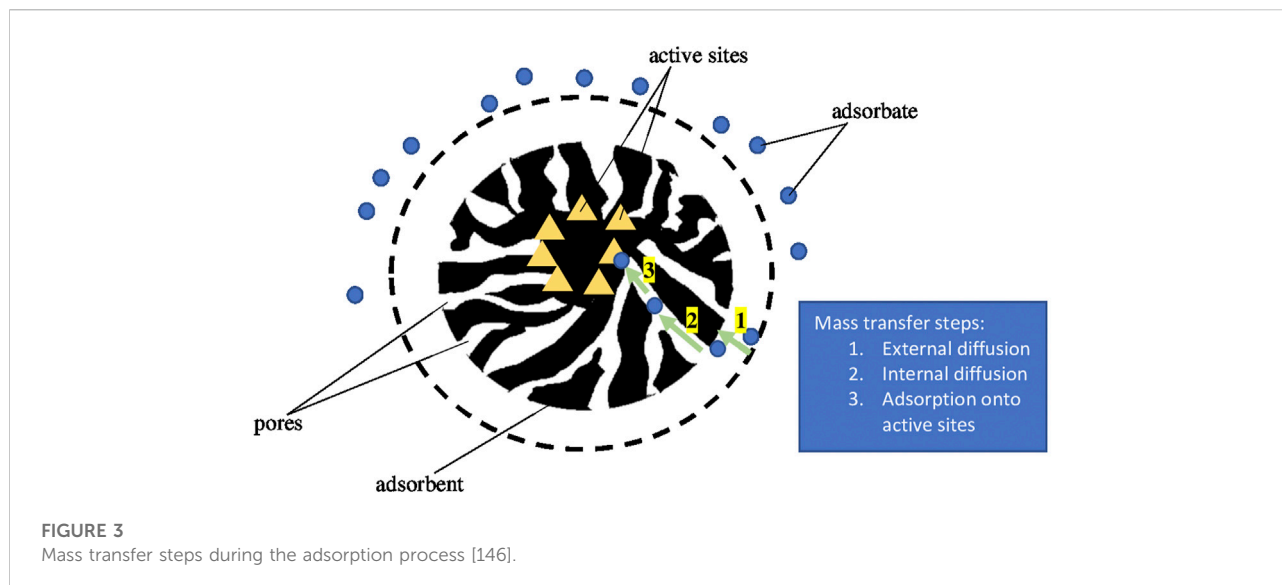
FIGURE 3
Mass transfer steps during the adsorption process [146].

on the adsorbent at an equilibrium state. Yan et al. (2017) stated that the adsorption isotherm verifies the performance of the adsorbent at the equilibrium state and constant temperature, which can be highly affected by several factors such as solution pH, solution temperature, and ionic strength. According to Ewis and Hameed (2021), increasing the concentration of the adsorbate can affect the nature of the adsorption process due to an increase in the adsorbate–adsorbent's effective collision, which accelerates the process. An isotherm model can be applied by plotting a curve between adsorbate molecules in the solid phase with the concentration of adsorbate molecules in the bulk phase, or pressure, in the cases of a liquid adsorption system and gas adsorption system, respectively (Al-Ghouti and Da'ana, 2020).

The adsorbate–adsorbent interaction for different adsorption systems is unique and unlike one another. Therefore, in the literature, a variety of isotherm models with different parameters are utilized to comprehend different adsorption systems. However, the most utilized ones in the studies involve textile dye adsorption onto a DPR-based adsorbent were Langmuir, Freundlich, Temkin, Dubinin–Radushkevich (D-R), Langmuir–Freundlich, and Redlich–Peterson models. These equations are provided in Table 7.

In a study conducted by Khadhri et al. (2019), the adsorption of indigo carmine dye onto date palm petiole-based AC followed the Langmuir model with a monolayer maximum adsorption capacity, Q_m, of 53.76 mg/g and a dimensionless separation factor, R_L, between 0.003 and 0.050. The Langmuir model was first invented to describe gas adsorption onto a solid adsorbent (Foo and Hameed, 2010). This model depicts monolayer coverage of an adsorbate onto the surface of an adsorbent, a process which operates based on the kinetic principle where the

rate of adsorption and desorption is equal in magnitude (Langmuir, 1916). Furthermore, this model also signifies that the surface of the adsorbent is filled with active sites that are distributed uniformly (Pal et al., 2018). Q_m is the maximum monolayer coverage and has been used extensively by researchers as a key indicator to measure adsorbents' performance and to compare the performance between one adsorbent and another. Meanwhile, the value of R_L is crucial to forecast the feasibility of the adsorption process. Different values of R_L can be interpreted differently as follows: favorable adsorption ($0 < R_L < 1$), unfavorable adsorption ($R_L > 1$), linear adsorption ($R_L = 1$), and irreversible adsorption ($R_L = 0$) (Yusop et al., 2021b). A similar result was observed in a study performed by El Ouadrhiri et al. (2021) where date stone hydrochar (DSH) was utilized to adsorb methylene blue (MB) and methyl orange (MO) dyes. Both MB-DSH and MO-DSH adsorption systems were found to follow the Langmuir isotherm the best with Q_m values of 657.89 and 384.61 mg/g, respectively, and R_L values of 0.01–0.29 and 0.004–0.010, respectively. El Ouadrhiri et al. (2021) pointed out that the adsorption of MB onto DSH was contributed by electrostatic attraction, π–π interaction, or n–π interaction whereas hydrogen bonds and hydrophobic interactions were responsible in the case of the MO-DSH system. Throughout the literature, a majority of the adsorbate-DPR-based adsorbents were disclosed to follow the Langmuir isotherm model the best. These systems include BRSM-date palm rachis-based AC (Daoud et al., 2017), methylene blue-date stone-based AC (Abbas and Ahmed, 2016), crystal violet-date stone-based AC (Messaoudi et al., 2016), and methylene blue-date stone-based AC (Foo and Hameed, 2011; Messaoudi et al., 2016).

The adsorption of methylene blue dye onto date palm leaf-based AC was found to follow the Freundlich model with 1/n

TABLE 7 Summary of common isotherm models used in adsorption systems that involved date palm residues.

Isotherm models	Important parameters	References
Langmuir $q_e = \frac{Q_m K_L C_e}{1+K_L C_e}$ (1)	Q_m = maximum monolayer adsorption capacity (mg/g)	Langmuir, (1918)
Freundlich $q_e = K_F C_e^{1/n_F}$ (2)	K_F = parameter related to adsorbed quantity ((mg/g) (L/mg)$^{1/n}$)	Freundlich, (1906)
	n = parameter related to adsorption strength	
Temkin $q_e = \frac{RT}{B} \ln(AC_e)$ (3)	A = equilibrium binding constant (L/g)	Temkin and Pyzhev, (1940)
	B = adsorption heat constant	
$B = \frac{RT}{b_T}$ (4)	b_T = Temkin constant (J/mol.K)	
Dubinin–Radushkevich (D-R)	Q_{DR} = maximum adsorbed adsorbate (mg/g)	Dubinin and Radushkevich, (1947)
$q_e = Q_{DR} - R^{e^{-K_{DR}\varepsilon^2}}$ (5)	K_{DR} = model constant (mol^2/kJ^2)	
$\varepsilon = RT \ln\frac{C_s}{C_e}$ (6)	ε = adsorption potential related to Polanyi's potential theory (kJ/mol)	
	Cs = solubility of adsorbates (mg/L)	
$E = \frac{1}{\sqrt{2K_{DR}}}$ (7)	E = mean free energy (kJ/mol)	
Langmuir–Freundlich	K_{LF} = equilibrium constant for heterogeneous solids	Sips, (1948)
$q_e = \frac{Q_m(K_{LF}C_e)^{m_{LF}}}{(1+(K_{LF}C_e)^{m_{LF}})}$ (8)	m_{LF} = heterogeneity parameter (lies between 0 and 1)	
Redlich–Peterson	K_R = R-P constant (L/mg)	Redlich and Peterson, (1959)
$q_e = \frac{K_R C_e}{1+A_R C_e^{\gamma}}$ (9)	A_R = R-P constant (L/mg)	
	Υ = R-P constant (value between 1 and 0)	

value of 0.22 and K_F value of 168.50 mg/g (L/mg)$^{1/n}$ (Shafiq et al., 2019). Other adsorption systems that were best described by the Freundlich isotherm were methylene blue-date seed-based AC (Islam et al., 2015) and maxilon blue-date stone-based AC (Alqaragully, 2014). The Freundlich model suggests multilayer sorption on the heterogeneous surface of the adsorbent. This model also proposes that numerous active sites are occupied at the initial state and as more sites are occupied, the activity becomes lower. Unlike the Langmuir model, the adsorption energy and affinity of adsorbates in the Freundlich model do not have to be evenly scattered on the heterogeneous surface of the adsorbent. Other assumptions in developing this model include: 1) different concentrations of the adsorbate solution resulted in an inconsistent ratio of the adsorbed adsorbate to the mass of the adsorbent and 2) upon completion of the adsorption process, the adsorption energy is decreased exponentially (Al-Ghouti and Da'ana, 2020). The parameter of n in this model can be used to determine the adsorption intensity. For instance, if the value of 1/n is between 0 and 1, it signifies favorable adsorption. On the contrary, if 1/n values become 1 and greater than 1, it corresponds to an irreversible process and unfavorable process, respectively. Islam et al. (2015) also found that the K_F value decreased as the solution temperature increased from 30 to 50°C, thus signifying the exothermic nature of that adsorption process. In addition, the physical bonding that was known to be the backbone of the Freundlich model became weaker at a higher solution temperature. Furthermore, the solubility of the dye increased at a higher solution temperature, making their tendency to escape from

the solid phase easier. On the contrary, Messaoudi et al. (2016) revealed that the adsorption of methylene blue and crystal violet dyes onto date stone-based AC caused an increase in K_F values when the solution temperature increased, thus resembling an endothermic type of adsorption process.

Several studies revealed that some adsorbate–adsorbents systems produced high R^2 values for both Langmuir and Freundlich models, which signified that those adsorption systems can be well-described by two isotherm models (Daoud et al., 2017; El Ouadrhiri et al., 2021). This phenomenon can be explained by the existence of both homogenous and heterogeneous types of surfaces on the adsorbent. Due to this, a model known as Langmuir–Freundlich was developed to cater for this type of adsorption system (Sips, 1948). At lower solute concentrations, this model tends to resolve to the Freundlich isotherm whereas at higher solute concentrations, this model becoming more of a Langmuir isotherm. In a study conducted by Hijab et al. (2021), malachite green dye adsorption onto date pit-based AC (produced via the conventional method) was found to follow the Langmuir–Freundlich isotherm. However, when the same precursor (date pits) was subjected to the microwave heating technique to adsorb the same adsorbate (malachite green), the adsorption data fitted the Redlich–Peterson isotherm model the best. Their study proved that the change in activation route can completely altered the adsorption behavior. Redlich-Peterson was built based on the theory of non-ideal monolayer adsorption where one active site could adsorb more than one adsorbate (Redlich

and Peterson, 1959; Hijab et al., 2021). This explained the higher adsorption capacity of the adsorption system that followed the Redlich–Peterson model (98.04 mg/g) as compared to the one that followed the Langmuir–Freundlich model (58.10 mg/g). The Redlich–Peterson isotherm was found to be excellent in describing the adsorption of multiples dyes onto date palm frond-based AC (Zubair et al., 2020b) and the adsorption of methyl orange dye onto date spathe-based AC (Emami and Azizian, 2014).

In addition to the classic isotherm models of Langmuir and Freundlich, Khadhri et al. (2019) and Shafiq et al. (2019) employed the Dubinin–Radushkevich (D-R) isotherm to fit the adsorption data. The D-R isotherm applied was found to be useful to determine the type of the sorption process that occurred. The parameter of mean energy of sorption, E, in this isotherm signifies physical adsorption when its value is below 8 kJ/mol and chemical adsorption when its value is greater than 8 kJ/mol (Gong et al., 2019). The Temkin isotherm model was found to be employed in several studies as well (Foo and Hameed, 2011; Alqaragully, 2014; Abbas and Ahmed, 2016; Daoud et al., 2017; Hijab et al., 2021). Out of these studies, only the study on the methyl orange-date stone-based AC adsorption system was found to follow the Temkin model (Alqaragully, 2014). This isotherm model considers the effect of the heat of adsorption together with the adsorbate–adsorbents interaction. The characteristics of the Temkin model includes 1) adsorption energy of all adsorbate molecules that form coverage on the adsorbent surface shows linear characteristics rather than a logarithmic one, 2) the endothermic nature of the adsorption process can be confirmed by the rise of the B value as the solution temperature increase (Aharoni and Ungarish, 1977), and 3) the value of B below 8 kJ represents physisorption whereas a value that is higher than 8 kJ denotes chemisorption (Isiuku and Nwabueze, 2019). A study conducted by Hijab et al. (2021) revealed that conventional heated-AC and microwave heated-AC were physisorption (B = 1.62 kJ/mol) and chemisorption (75.42 kJ/mol), respectively. Their study once again established the fact that different types of heat treatment can affect the nature of the adsorption process altogether. Similar findings where adsorption systems were best described by chemisorption (B value >8 kJ) were BRSM-date palm rachis-based AC (Daoud et al., 2017), methylene blue-date stone-based AC (Abbas and Ahmed, 2016), and methylene blue-date stone-based AC (Foo and Hameed, 2011). According to Al-Ghouti and Da'ana (2020), the Temkin model is efficient in predicting the adsorption equilibria in the gas phase but poorly appropriate in representing the aqueous phase adsorption process. It can be concluded that most textile dye-DPR-based AC

adsorption systems followed Langmuir, some studies followed Freundlich and Redlich–Peterson isotherms, very few followed Langmuir–Freundlich and Temkin isotherms, whereas none was observed to follow the D-R isotherm.

6.2 Adsorption kinetics

The study of adsorption kinetics is vital in providing useful information such as the rate of the adsorption process and the mechanisms of the mass transfer involved. Such information is beneficial in aiding the design and the scaling-up processes of the adsorption systems (Qureshi et al., 2020). According to Ahmed and Hameed (2019), a kinetic study enables the researchers to estimate the saturation time of the adsorbent used as well. There are three steps in kinetic mass transfer: 1) external diffusion (film diffusion) which involves the movement of adsorbate molecules through the liquid film around the adsorbent, 2) internal diffusion (pore diffusion) which relates to the diffusion of adsorbate molecules in the adsorbent's pores, and 3) sorption of the adsorbate molecules on the adsorbent's active sites which can either be physisorption or chemisorption. If physisorption is involved, then the researchers can employ the heat treatment method for a regeneration study. On the contrary, if chemisorption is involved, the better method to regenerate the exhausted adsorbent is through chemical solvent treatment. The kinetic behavior of the adsorption process can be evaluated by plotting the amount of adsorbate adsorbed against the contact time (Tan and Hameed, 2017).

In the literature, the most encountered kinetic models to model the adsorption process of textile dyes onto DPR-based AC were pseudo-first-order (PFO), pseudo-second-order (PSO), and Elovich and intraparticle diffusion. The PFO model was used to determine the involvement of physisorption in the adsorption process. Qureshi et al. (2020) observed that the chance for an adsorption process to obey this model is higher under longer contact time as the equilibrium state is about to be attained. According to Reddy et al. (2017), PFO and PSO are associated with physisorption and chemisorption, respectively. PFO is the best to predict the kinetic behavior of the adsorption system in the early stage whereas PSO is best used to predict the kinetic behavior of the prolonged adsorption system (Ho and McKay, 1999). It was stated by Prajapati and Mondal (2020) that PSO was built based on the assumption that functional groups on adsorbents play a major role in the adsorption process. Another kinetic model that is based on the dominance of chemisorption is Elovich, which was developed by assuming that the activation energy increases with the adsorption time and the adsorbent's surface is heterogeneous (Elovich and Larinov, 1962). Last but not least, intraparticle diffusion is known to be the widest method in verifying the routes in the adsorption process due to convenience of use. If the intraparticle diffusion plot passes through the origin point (0,0), then the rate-limiting step

TABLE 8 Summary of kinetic models employed in dye-DPR-based AC adsorption systems.

Kinetic models	Important parameters	References
Pseudo-first-order (PFO) $q_t = q_e (1 - e^{-k_1 t})$ (10)	k_1 = PFO rate constant (1/min)	Lagergren and Svenska, (1898)
Pseudo-second-order (PSO) $q_t = \frac{k_2 q_e^2 t}{1 + k_2 q_e t}$ (11)	k_2 = PSO rate constant (g/mg min)	Ho and McKay, (1998)
Elovich $q_t = \frac{1}{\beta} \ln(1 + \alpha \beta t)$ (12)	α = primary rate of adsorption (mg/g min) β = desorption parameter which corresponds to the activation energy and the level of chemisorption	Roginsky and Zeldovich, (1934)
Intraparticle diffusion $q_t = k_{di} t^{1/2} + C_i$ (13)	k_{di} = rate constant (mg/g.min$^{1/2}$) C_i = degree of adsorption	Weber and Morris, (1963)

is known to be the intraparticle diffusion. Contrary to this, then the rate-limiting step is contributed by several types of mechanisms (Weber and Morris, 1963). A summary of these kinetic equations is given in Table 8.

In a study to verify the adsorption performance of anionic and cationic dyes (methylene blue, crystal violet, Eriochrome black T, and methyl orange) onto date palm frond-based biochar, these systems were found to follow PSO due to a high R^2 value of >0.99, therefore signifying the role of chemisorption in these adsorption processes (Zubair et al., 2020b). The results of their study further suggested that the adsorption of dyes onto the biochar's surface involved pi–pi interactions, electrostatic interactions, and chemical reactions. The intraparticle diffusion model employed in their study revealed that the adsorption of cationic and anionic dyes is contributed by a variety of mechanisms, since the value of C is not equal to 0 (Zhu et al., 2018). Similar results were obtained in a study conducted by Shafiq et al. (2019) where the adsorption of methylene blue onto date palm leaf-based biochar was found to follow PSO due to high R^2 (>0.99). In fact, a perfect correlation (R^2 = 1) was noticed when the concentration of methylene blue was 100 and 150 mg/L, which indicated a strong role of chemisorption. Khadhri et al. (2019) found that the rate constant, k_2, decreased when indigo carmine concentration increased from 10 to 100 mg/L and then increased to 150 mg/L before decreasing back at 500 mg/L. This zig-zag pattern of k_2 gave an insight into the variety of mechanisms involved in that adsorption process. The influence of chemisorption was contributed by carboxylic groups (0.165 mmol/g), lactonic groups (0.179 mmol/g), phenolic groups (0.099 mmol/g), and total basic groups (0.756 mmol/g) that existed on the surface of the adsorbent.

Another study of the BRSM-date palm rachis-based AC adsorption system revealed that intraparticle diffusion played a role in the adsorption process but was not the only mechanism involved in the rate-limiting step, since the linear plots of intraparticle diffusion did not pass through the origin (Daoud et al., 2017). This hypothesis was supported by a wide range of R^2 obtained (0.62–0.99) which symbolized the

unfit correlation of the model and intraparticle diffusion model at a certain BRSM concentration. Other studies also showed that PSO > PFO (Ashour, 2010; Islam et al., 2015; Messaoudi et al., 2016) and PSO > PFO > intraparticle diffusion model (Abbas and Ahmed, 2016). Ashour (2010) revealed that PFO fitted kinetic data quite well (R^2 > 0.96) but failed to predict the experimental values of q_e with a low error. Moreover, the adsorption of dyes onto date pit-based AC can only be described by PFO within a limited range of contact time only. Similar results were observed in the studies of Eriochrome black T and methyl orange removal by date palm frond-based AC (Zubair et al., 2020b) where PFO gave relatively high R^2 values of 0.922 and 0.971, respectively, but poorly predicted the experimental values. The study performed by Emami and Azizian (2014) showed that the adsorption process fitted the kinetic models in the order of Elovich (R^2 > 0.9813) > PSO (R^2 > 0.9141 > PFO (R^2 > 0.8108). This result proved that the surface of date spathe-based AC was heterogeneous and the adsorption process was governed by chemisorption, which was aided by an abundant number of active sites. The supremacy of PSO in fitting a majority of adsorption systems as compared to PFO is known to be rooted in a theoretical basis instead of a physical one (Plazinski et al., 2009). As discussed in the previous section (characteristics of DPR), DPR was revealed to be naturally rich in different kinds of functional groups. These functional groups fueled the chemisorption interaction during dye adsorption onto DPR-based AC. The employment of PSO seems to be more convenient than PFO, since equilibrium adsorption capacity, q_e, is not necessary for data fitting (Qureshi et al., 2020). Table 9 shows the summary of isotherm and kinetic models for textile dye removal by DPR-based AC.

7 Future trends

Date palm residue (DPR)-based AC demonstrated a competitive performance compared to other types of biomass-based AC when it comes to treating textile dye

TABLE 9 Summary of isotherm and kinetic models for textile dye removal by date palm residue-based activated carbons.

Precursor	Type of carbonization	Type of activation	Adsorbate (dyes)	Isotherm	Kinetic	References
Date pits	Pyrolysis	Chemical	Malachite green	Langmuir–Freundlich	-	Hijab et al. (2021)
Date pits	Microwave heating	Chemical	Malachite green	Redlich–Peterson	-	Hijab et al. (2021)
Date stones	Hydrothermal	Chemical	Methylene blue	Langmuir	-	El Ouadrhiri et al. (2021)
Date stones	Hydrothermal	Chemical	Methyl orange	Langmuir	-	El Ouadrhiri et al. (2021)
Date palm fronds	Pyrolysis	-	Methylene blue	Redlich–Peterson	PSO	Zubair et al. (2020b)
Date palm fronds	Pyrolysis	-	Crystal violet	Redlich-Peterson	PSO	Zubair et al. (2020b)
Date palm fronds	Pyrolysis	-	Eriochrome black T	Redlich–Peterson	PSO	Zubair et al. (2020b)
Date palm fronds	Pyrolysis	-	Methyl orange	Redlich–Peterson	PSO	Zubair et al. (2020b)
Date palm petiole	Pyrolysis	Chemical	Indigo carmine	Langmuir	PSO	Khadhri et al. (2019)
Date palm leaves	Pyrolysis	-	Methylene blue	Freundlich	PSO	Shafiq et al. (2019)
Date palm rachis	Chemical	Pyrolysis	Bezaktiv Red S-Max	Langmuir	PSO	Daoud et al. (2017)
Date stones	Chemical	Microwave heating	Methylene blue	Langmuir	PSO	Abbas and Ahmed, (2016)
Date stones	Chemical	Pyrolysis	Methylene blue	Langmuir	PSO	Messaoudi et al. (2016)
Date stones	Chemical	Pyrolysis	Crystal violet blue	Langmuir	PSO	Messaoudi et al. (2016)
Date palm seed	Hydrothermal	Chemical	Methylene blue	Freundlich	PSO	Islam et al. (2015)
Date spathe	Chemical	Microwave heating	Methyl orange	Redlich–Peterson	Elovich	Emami and Azizian, (2014)
Date stones	Chemical	Pyrolysis	Methyl orange	Temkin	-	Alqaragully, (2014)
Date stones	Chemical	Pyrolysis	Maxilon blue	Freundlich	-	Alqaragully, (2014)
Date stones	Pyrolysis	Chemical + microwave heating	Methylene blue	Langmuir	-	Foo and Hameed, (2011)

wastewater. However, several issues need to be addressed by researchers to further improve the research relevance of such adsorption processes. First and foremost, all adsorption studies were conducted *via* the batch mode, which is quite difficult to be implemented in the industry. It is suggested for researchers to explore the performance of textile dye-DPR-based AC adsorption systems through a continuous column study as this mode is more practical to be used at a larger scale. Second, various synthetic chemicals were used to activate DPR and the fate of these chemicals at the end of the washing step was unknown. Although some of them are approved by the FDA as safe to be used, the accumulation of these chemicals in open water sources at high consistency can still affect aquatic life. Therefore, it is suggested to use natural chemicals such as lemon juice (Khan T. M. et al., 2019) and calcium carbonite derived from seashells. Also, it is highly recommended for researchers to adopt an optimization study to determine the exact optimum impregnation ratio (IR) between the sample and chemicals used so that no excess chemicals are wasted, thus preventing the AC's total cost of production to increase. Innovation in using chemicals to activate samples should be made so that their usage can be kept at a bare minimum, such as using chemicals only to modify the surface of the sample. Third, focus on the adsorption performance of DPR-based AC in removing multi-component of dyes is noticed. The majority only focused

on a single system whereas some focused on a binary mixture. In the real world, it is common for effluents from textile industries to contain more than one type of dyes. It was also noted that all studies used synthetic dye wastewater and not real textile industry wastewater. Real textile industry wastewater posed a more challenging task to be treated since it comprises many other components in addition to dyes; therefore, utilizing them as adsorbates can yield more accurate information regarding the potential of DPR-based AC as adsorbents. Fourth, AC derived from DPR posed a relatively brittle and less durable structure, which led to the limitation in the regeneration process *via* physical activation. It is suggested to combine DPR with a polymer to improve its physical strength. Fifth, after carbonization and activation processes took place, certain functional groups on DPR-based AC were found to be diminished, thus reducing the adsorption capacity of the adsorbent. It is recommended to calcinate the DPR-based AC with metal salts (copper or ferum) to introduce new functional groups on the adsorbents, thus enhancing the adsorption capacity. Lastly, only classic isotherm models (Langmuir, Freundlich, and Temkin) and kinetic models (PFO, PSO, and intraparticle diffusion) were used; thus, only limited information can be obtained. It is suggested for researchers to use other isotherm models (Dubinin–Radushkevich, Sips, Koble–Corrigan, and Toth) and kinetic models (Boyd plot, Elovich, and Avrami) so that the adsorption process can be better understood.

8 Conclusion

The technologies to produce AC from date palm residues (DPR) and their adsorption performance as an adsorbent in adsorbing a wide range of textile dyes had been reviewed. It was found that almost every part of DPR (date stones, date palm leaf, date palm fronds, and date palm fibers) have been successfully utilized by researchers to remove harmful textile dyes. The conversion of DPR into AC *via* different types of carbonization processes (pyrolysis or hydrothermal) and activation processes (physical, chemical, and physicochemical) were found to produce AC with different physical and chemical properties which were efficient in adsorbing the molecularly complex textile dyes. The majority of the dye-DPR-based AC adsorption systems were found to follow the Langmuir isotherm with competitive values of maximum monolayer coverage. The finding of the isotherm study was supported by the result in the kinetic study where most adsorption systems were found to follow pseudo-second-order (PSO), therefore signifying the role of chemisorption in the adsorption process. This was contributed by the chemical interactions between the ions of textile dyes and the polar functional groups which were widely scattered on the surface of DPR-based AC. In conclusion, DPR was found to be a good precursor for AC production, and DPR-based AC showed good adsorption performance in adsorbing textile dyes, which is comparable to the performance of commercial AC. The conversion of DPR to AC can solve the disposal problem of DPR, increase the economic value of DPR, reducing the world's dependency on non-renewable feedstock such as coal, and most importantly, to promote the sustainability concept for a better future.

Author contributions

HA: conceptualization, synthesis of published information, and writing the first draft of the manuscript. BH: conceptualization, development of the review outlines, and writing—review and editing. KA: funding acquisition, project administration, and writing—review and editing. SA: writing—review and editing. AA: writing—review and editing. The final version of the manuscript was approved by all authors.

Conflict of interest

The authors declare that the research was conducted in the absence of any commercial or financial relationships that could be construed as a potential conflict of interest.

Publisher's note

All claims expressed in this article are solely those of the authors and do not necessarily represent those of their affiliated organizations, or those of the publisher, the editors, and the reviewers. Any product that may be evaluated in this article, or claim that may be made by its manufacturer, is not guaranteed or endorsed by the publisher.

References

Abbas, A., Ahmed, M., and Darweesh, T. (2016). Adsorption of fluoroquinolones antibiotics on activated carbon by K2CO3 with microwave assisted activation. *Iraqi J. Chem. Petroleum Eng.* 17, 15–23.

Abbas, A. F., and Ahmed, M. J. (2016). Mesoporous activated carbon from date stones (Phoenix dactylifera L.) by one-step microwave assisted K2CO3 pyrolysis. *J. Water Process Eng.* 9, 201–207. doi:10.1016/j.jwpe.2016.01.004

Abd El-Monaem, E. M., Omer, A. M., El-Subruiti, G. M., Mohy-Eldin, M. S., and Eltaweil, A. S. (2022). Zero-valent iron supported-lemon derived biochar for ultra-fast adsorption of methylene blue. *Biomass Convers. biorefin.* doi:10.1007/s13399-022-02362-y

Aharoni, C., and Ungarish, M. (1977). Kinetics of activated chemisorption. Part 2.—theoretical models. *J. Chem. Soc. Faraday Trans.* 73, 456–464. doi:10.1039/F19777300456

Ahmad, M. A., AswarEusoff, M., Oladoye, P. O., Adegok, K. A., and Bell, O. S. (2021). Optimization and batch studies on adsorption of Methylene blue dye using pomegranate fruit peel based adsorbent. *Chem. Data Collect.* 32, 100676. doi:10.1016/j.cdc.2021.100676

Ahmad, T., Danish, M., Rafatullah, M., Ghazali, A., Sulaiman, O., Hashim, R., et al. (2011). The use of date palm as a potential adsorbent for wastewater treatment: A review. *Environ. Sci. Pollut. Res.* 19, 1464–1484. doi:10.1007/s11356-011-0709-8

Ahmed, M. J., and Hameed, B. H. (2019). Insights into the isotherm and kinetic models for the coadsorption of pharmaceuticals in the absence and presence of metal ions: A review. *J. Environ. Manag.* 252, 109617. doi:10.1016/j.jenvman.2019.109617

Al-Alawi, R. A., Al-Mashiqri, J. H., Al-Nadabi, J. S. M., Al-Shihi, B. I., and Baqi, Y. (2017). Date palm tree (Phoenix dactylifera L.): Natural products and therapeutic options. *Front. Plant Sci.* 8 (845). doi:10.3389/fpls.2017.00845

Al-Farsi, M., Alasalvar, C., Morris, A., Baron, M., and Shahidi, F. (2005). Comparison of antioxidant activity, anthocyanins, carotenoids, and phenolics of three native fresh and sun-dried date (Phoenix dactylifera L.) varieties grown in Oman. *J. Agric. Food Chem.* 53 (19), 7592–7599. doi:10.1021/jf050579q

Al-Ghouti, M. A., and Da'ana, D. A. (2020). Guidelines for the use and interpretation of adsorption isotherm models: A review. *J. Hazard. Mater.* 393, 122383. doi:10.1016/j.jhazmat.2020.122383

Al-Harrasi, A., Rehman, N. U., Hussain, J., Khan, A. L., Al-Rawahi, A., Gilani, S. A., et al. (2014). Nutritional assessment and antioxidant analysis of 22 date palm (Phoenix dactylifera) varieties growing in Sultanate of Oman. *Asian pac. J. Trop. Med.* 7s1, S591–S598. doi:10.1016/s1995-7645(14)60294-7

Alimohammadi, P., Shahabi Nejad, M., Miroliaei, M. R., and Sheibani, H. (2022). Oriented growth of copper & nickel-impregnated δ-MnO2 nanofilaments anchored onto sulfur-doped biochar template as hybrid adsorbents for removing phenolic compounds by adsorption-oxidation process. *Chem. Eng. Process. - Process Intensif.* 176, 108971. doi:10.1016/j.cep.2022.108971

Alqaragully, M. B. (2014). Removal of textile dyes (maxilon blue, and methyl orange) by date stones activated carbon. *Int. J. Adv. Res. Chem. Sci.* 1 (1), 48–59.

Ashour, S. S. (2010). Kinetic and equilibrium adsorption of methylene blue and remazol dyes onto steam-activated carbons developed from date pits. *J. Saudi Chem. Soc.* 14 (1), 47–53. doi:10.1016/j.jscs.2009.12.008

Barani, H., and Maleki, H. (2020). Red cabbage anthocyanins content as a natural colorant for obtaining different color on wool fibers. *Pigment Resin Technol.* 49 (3), 229–238. doi:10.1108/PRT-09-2019-0080

Barani, H., Rezaee, K., and Maleki, H. (2019). Influence of dyeing conditions of natural dye extracted from Berberis integerrima fruit on color shade of woolen yarn. *J. Nat. Fibers* 16 (4), 524–535. doi:10.1080/15440478.2018.1427172

Basheer, A. O., Hanafiah, M. M., Alsaadi, M. A., Al-Douri, Y., and Al-Raad, A. A. (2021). Synthesis and optimization of high surface area mesoporous date palm fiber-based nanostructured powder activated carbon for aluminum removal. *Chin. J. Chem. Eng.* 32, 472–484. doi:10.1016/j.cjche.2020.09.071

Basheer, O., Hanafiah, A., M., Abdulhakim Alsaadi, M., Al-Douri, Y., Malek, M. A., Mohammed Aljumaily, et al. (2019). Synthesis and characterization of natural extracted precursor date palm fibre-based activated carbon for aluminum removal by RSM optimization. *Process. (Basel).* 7 (5), 249. doi:10.3390/pr7050249

Bastidas-Oyanedel, J.-R., Fang, C., Almardeai, S., Javid, U., Yousuf, A., and Schmidt, J. E. (2016). Waste biorefinery in arid/semi-arid regions. *Bioresour. Technol.* 215, 21–28. doi:10.1016/j.biortech.2016.04.010

Behar, F., Lewan, M. D., Lorant, F., and Vandenbroucke, M. J. (2003). Comparison of artificial maturation of lignite in hydrous and nonhydrous conditions. *Org. Geochem.* 34, 575–600. doi:10.1016/s0146-6380(02)00241-3

Ben Salem, I., El Gamal, M., Sharma, M., Hameedi, S., and Howari, F. M. (2021). Utilization of the UAE date palm leaf biochar in carbon dioxide capture and sequestration processes. *J. Environ. Manag.* 299, 113644. doi:10.1016/j.jenvman.2021.113644

Benavente, V., Calabuig, E., and Fullana, A. (2015). Upgrading of moist agro-industrial wastes by hydrothermal carbonization. *J. Anal. Appl. Pyrolysis* 113, 89–98. doi:10.1016/j.jaap.2014.11.004

Benkhaya, S., M' rabet, S., and El Harfi, A. (2020). A review on classifications, recent synthesis and applications of textile dyes. *Inorg. Chem. Commun.* 115, 107891. doi:10.1016/j.inoche.2020.107891

Bensidhom, G., Ben Hassen-Trabelsi, A., Alper, K., Sghairoun, M., Zaafouri, K., and Trabelsi, I. (2018). Pyrolysis of Date palm waste in a fixed-bed reactor: Characterization of pyrolytic products. *Bioresour. Technol.* 247, 363–369. doi:10.1016/j.biortech.2017.09.066

Berradi, M., Hsissou, R., Khudhair, M., Assouag, M., Cherkaoui, O., El Bachiri, A., et al. (2019). Textile finishing dyes and their impact on aquatic environs. *Heliyon* 5 (11), e02711. doi:10.1016/j.heliyon.2019.e02711

Borghol, Y., El-Kady, M. Y., Khalil, M. H., El-Malky, M., and Abd Elatif, A. A. (2019). Using of date palm leaf midrib biochar as an adsorbant in water treatment. *J. Environ. Sci.* 48 (3), 1–20. doi:10.21608/jes.2019.160146

Bouchemal, N., Azoudj, Y., Zoulikha, M., and Addoun, F. (2012). Adsorption modeling of Orange G dye on mesoporous activated carbon prepared from Algerian date pits using experimental designs. *Desalination Water Treat.* 45, 284–290. doi:10.1080/19443994.2012.692042

Braghiroli, F. L., Bouafif, H., and Koubaa, A. (2019). Enhanced SO2 adsorption and desorption on chemically and physically activated biochar made from wood residues. *Industrial Crops Prod.* 138, 111456. doi:10.1016/j.indcrop.2019.06.019

Burkinshaw, S. M., and Salihu, G. (2019). The role of auxiliaries in the immersion dyeing of textile fibres: Part 6 analysis of conventional models that describe the manner by which inorganic electrolytes promote reactive dye uptake on cellulosic fibres. *Dyes Pigments* 161, 595–604. doi:10.1016/j.dyepig.2017.09.028

Chahinez, H.-O., Abdelkader, O., Leila, Y., and Tran, H. N. (2020). One-stage preparation of palm petiole-derived biochar: Characterization and application for adsorption of crystal violet dye in water. *Environ. Technol. Innovation* 19, 100872. doi:10.1016/j.eti.2020.100872

Chao, C. T., and Krueger, R. R. (2007). The date palm (Phoenix dactylifera L.): Overview of biology, uses, and cultivation. *HortScience* 42 (5), 1077–1082. doi:10.21273/hortsci.42.5.1077

Chaudhary, M., Suhas, Singh, R., Tyagi, I., Ahmed, J., Chaudhary, S., et al. (2021). Microporous activated carbon as adsorbent for the removal of noxious anthraquinone acid dyes: Role of adsorbate functionalization. *J. Environ. Chem. Eng.* 9 (5), 106308. doi:10.1016/j.jece.2021.106308

Chaves Fernandes, B. C., Ferreira Mendes, K., Dias Júnior, A. F., da Silva Caldeira, V. P., da Silva Teófilo, T. M., Severo Silva, T., et al. (2020). Impact of pyrolysis temperature on the properties of Eucalyptus wood-derived biochar. *Materials* 13 (24), 5841. doi:10.3390/ma13245841

Chu, G., Zhao, J., Huang, Y., Zhou, D., Liu, Y., Wu, M., et al. (2018). Phosphoric acid pretreatment enhances the specific surface areas of biochars by generation of micropores. *Environ. Pollut.* 240, 1–9. doi:10.1016/j.envpol.2018.04.003

Daoud, M., Benturki, O., Kecira, Z., Girods, P., and Donnot, A. (2017). Removal of reactive dye (BEZAKTIV Red S-MAX) from aqueous solution by adsorption onto activated carbons prepared from date palm rachis and jujube stones. *J. Mol. Liq.* 243, 799–809. doi:10.1016/j.molliq.2017.08.093

Dawson, E. A., Parkes, G. M. B., Barnes, P. A., Bond, G., and Mao, R. (2008). The generation of microwave-induced plasma in granular active carbons under fluidised bed conditions. *Carbon* 46 (2), 220–228. doi:10.1016/j.carbon.2007.11.004

Dehghani, M. H., Mahmoodi, M., and Zarei, A. (2019). Toxicity study of UV/ZnO treated solution containing Reactive blue 29 using Daphnia magna as a biological indicator. *MethodsX* 6, 660–665. doi:10.1016/j.mex.2019.03.019

Dubinin, M. M., and Radushkevich, L. V. (1947). The equation of the characteristic curve of the activated charcoal. *Proc. Acad. Sci. USSR Phys. Chem. Sect.* 55, 331–337.

El Bassam, N. (2010). *Handbook of bioenergy crops: A complete reference to species, development and applications.* 1st ed. London, United Kingdom: Routledge.

El Marouani, M., Azoulay, K., Bencheikh, I., El Fakir, L., Rghioui, L., El Hajji, A., et al. (2018). Application of raw and roasted date seeds for dyes removal from aqueous solution. *J. Mater. Environ. Sci.* 9, 2387–2396.

El Ouadrhiri, F., Elyemni, M., Lahkimi, A., Lhassani, A., Chaouch, M., and Taleb, M. (2021). Mesoporous carbon from optimized date stone hydrochar by catalytic hydrothermal carbonization using response surface methodology: Application to dyes adsorption. *Int. J. Chem. Eng.* 2021, 1–16. doi:10.1155/2021/5555406

El-Bindary, M. A., El-Desouky, M. G., and El-Bindary, A. A. (2022). Adsorption of industrial dye from aqueous solutions onto thermally treated green adsorbent: A complete batch system evaluation. *J. Mol. Liq.* 346, 117082. doi:10.1016/j.molliq.2021.117082

El-Juhany, L. (2010). Degradation of date palm trees and date production in Arab countries: Causes and potential rehabilitation. *Aust. J. Basic Appl. Sci.* 4, 3998–4010.

Elovich, S. Y., and Larinov, O. (1962). Theory of adsorption from solutions of non electrolytes on solid (I) equation adsorption from solutions and the analysis of its simplest form, (II) verification of the equation of adsorption isotherm from solutions. *J. Izv. Akad. Nauk. SSSR, Otd. Khim. Nauk.* 2 (2), 209–216.

Eltaweil, A. S., Abd El-Monaem, E. M., Elshishini, H. M., El-Aqapa, H. G., Hosny, M., Abdelfatah, A. M., et al. (2022). Recent developments in alginate-based adsorbents for removing phosphate ions from wastewater: A review. *RSC Adv.* 12 (13), 8228–8248. doi:10.1039/D1RA09193J

Emami, Z., and Azizian, S. (2014). Preparation of activated carbon from date sphate using microwave irradiation and investigation of its capability for removal of dye pollutant from aqueous media. *J. Anal. Appl. Pyrolysis* 108, 176–184. doi:10.1016/j.jaap.2014.05.002

Eoin, L. N. (2016). Systematics: Blind dating. *Nat. Plants* 2 (5), 16069. doi:10.1038/nplants.2016.69

Espro, C., Satira, A., Mauriello, F., Anajafi, Z., Moulaee, K., Iannazzo, D., et al. (2021). Orange peels-derived hydrochar for chemical sensing applications. *Sensors Actuators B Chem.* 341, 130016. doi:10.1016/j.snb.2021.130016

Ewis, D., and Hameed, B. H. (2021). A review on microwave-assisted synthesis of adsorbents and its application in the removal of water pollutants. *J. Water Process Eng.* 41, 102006. doi:10.1016/j.jwpe.2021.102006

Foo, K. Y., and Hameed, B. H. (2010). Insights into the modeling of adsorption isotherm systems. *Chem. Eng. J.* 156 (1), 2–10. doi:10.1016/j.cej.2009.09.013

Foo, K. Y., and Hameed, B. H. (2011). Preparation of activated carbon from date stones by microwave induced chemical activation: Application for methylene blue adsorption. *Chem. Eng. J.* 170 (1), 338–341. doi:10.1016/j.cej.2011.02.068

Freundlich, H. M. F. (1906). Over the adsorption in solution. *J. Phys. Chem.* 57, 385–471.

Funke, A., and Ziegler, F. (2010). Hydrothermal carbonization of biomass: A summary and discussion of chemical mechanisms for process engineering. *Biofuel. Bioprod. Biorefin.* 4 (2), 160–177. doi:10.1002/bbb.198

Ge, S., Foong, S. Y., Ma, N. L., Liew, R. K., Wan Mahari, W. A., Xia, C., et al. (2020). Vacuum pyrolysis incorporating microwave heating and base mixture modification: An integrated approach to transform biowaste into eco-friendly bioenergy products. *Renew. Sustain. Energy Rev.* 127, 109871. doi:10.1016/j.rser.2020.109871

Gita, S., Shukla, S. P., Saharan, N., Prakash, C., and Deshmukhe, G. (2019). Toxic effects of selected textile dyes on elemental composition, photosynthetic pigments, protein content and growth of a freshwater chlorophycean alga Chlorella vulgaris. *Bull. Environ. Contam. Toxicol.* 102 (6), 795–801. doi:10.1007/s00128-019-02599-w

Gong, W., Jiang, M., Han, P., Liang, G., Zhang, T., and Liu, G. (2019). Comparative analysis on the sorption kinetics and isotherms of fipronil on nondegradable and biodegradable microplastics. *Environ. Pollut.* 254, 112927. doi:10.1016/j.envpol.2019.07.095

Graber, E. R., Meller Harel, Y., Kolton, M., Cytryn, E., Silber, A., Rav David, D., et al. (2010). Biochar impact on development and productivity of pepper and tomato grown in fertigated soilless media. *Plant Soil* 337 (1), 481–496. doi:10.1007/s11104-010-0544-6

Gregoriou, S., Mastraftsi, S., Hatzidimitriou, E., Tsimpidakis, A., Nicolaidou, E., Stratigos, A., et al. (2020). "Occupational and non-occupational allergic contact dermatitis to hair dyes in Greece. A 10-year retrospective study. *Contact derm.*, 83, 277–285. doi:10.1111/cod.13598

Guo, G., Tian, F., Zhang, L., Ding, K., Yang, F., Hu, Z., et al. (2020). Effect of salinity on removal performance in hydrolysis acidification reactors treating textile wastewater. *Bioresour. Technol.* 313, 123652. doi:10.1016/j.biortech.2020.123652

Haeldermans, T., Campion, L., Kuppens, T., Vanreppelen, K., Cuypers, A., and Schreurs, S. (2020). A comparative techno-economic assessment of biochar production from different residue streams using conventional and microwave pyrolysis. *Bioresour. Technol.* 318, 124083. doi:10.1016/j.biortech.2020.124083

Haghbin, M. R., and Niknam Shahrak, M. (2021). Process conditions optimization for the fabrication of highly porous activated carbon from date palm bark wastes for removing pollutants from water. *Powder Technol.* 377, 890–899. doi:10.1016/j.powtec.2020.09.051

Haji, A., and Naebe, M. (2020). Cleaner dyeing of textiles using plasma treatment and natural dyes: A review. *J. Clean. Prod.* 265, 121866. doi:10.1016/j.jclepro.2020.121866

Haque, K. E. (1999). Microwave energy for mineral treatment processes—A brief review. *Int. J. Mineral Process.* 57 (1), 1–24. doi:10.1016/S0301-7516(99)00009-5

Hassan, M. M., and Carr, C. M. (2018). A critical review on recent advancements of the removal of reactive dyes from dyehouse effluent by ion-exchange adsorbents. *Chemosphere* 209, 201–219. doi:10.1016/j.chemosphere.2018.06.043

Hassan, S. S. M., Awwad, N. S., and Aboterika, A. H. A. (2009). Removal of synthetic reactive dyes from textile wastewater by Sorel's cement. *J. Hazard. Mater.* 162 (2), 994–999. doi:10.1016/j.jhazmat.2008.05.138

Hazzouri, K. M., Flowers, J. M., Visser, H. J., Khierallah, H. S. M., Rosas, U., Pham, G. M., et al. (2015). Whole genome re-sequencing of date palms yields insights into diversification of a fruit tree crop. *Nat. Commun.* 6, 8824. doi:10.1038/ncomms9824

He, J., Ren, S., Zhang, S., and Luo, G. (2021). Modification of hydrochar increased the capacity to promote anaerobic digestion. *Bioresour. Technol.* 341, 125856. doi:10.1016/j.biortech.2021.125856

Hihara, T., Okada, Y., and Morita, Z. (2002). Photo-oxidation and -reduction of vat dyes on water-swollen cellulose and their lightfastness on dry cellulose. *Dyes Pigments* 53 (2), 153–177. doi:10.1016/S0143-7208(02)00017-7

Hijab, M., Parthasarathy, P., Mackey, H. R., Al-Ansari, T., and McKay, G. (2021). Minimizing adsorbent requirements using multi-stage batch adsorption for malachite green removal using microwave date-stone activated carbons. *Chem. Eng. Process. - Process Intensif.* 167, 108318. doi:10.1016/j.cep.2021.108318

Hijab, M. S., Parthasarathy, P., Li, P., Mackey, H. R., Al-Ansari, T., Mohammed, R. R., et al. (2020). Active carbon from microwave date stones for toxic dye removal: Setting the design capacity. *Chem. Eng. Technol.* 43 (9), 1841–1849. doi:10.1002/ceat.202000059

Ho, Y.-S., and McKay, G. (1998). Sorption of dye from aqueous solution by peat. *Chem. Eng. J.* 70 (2), 115–124. doi:10.1016/s0923-0467(98)00076-1

Ho, Y. S., and McKay, G. (1999). Pseudo-second order model for sorption processes. *Process Biochem.* 34 (5), 451–465. doi:10.1016/S0032-9592(98)00112-5

Hoseinzadeh Hesas, R., Ashri Wan Daud, W. M., Sahu, J., and Arami Niya, A. (2012). The effects of a microwave heating method on the production of activated carbon from agricultural waste: A review. *J. Anal. Appl. Pyrolysis* 100, 1–11. doi:10.1016/j.jaap.2012.12.019

Hu, B., Wang, K., Wu, L., Yu, S.-H., Antonietti, M., and Titirici, M.-M. (2010). Engineering carbon materials from the hydrothermal carbonization process of biomass. *Adv. Mat.* 22 (7), 813–828. doi:10.1002/adma.200902812

Huang, Y.-F., Chiueh, P.-T., and Lo, S.-L. (2016). A review on microwave pyrolysis of lignocellulosic biomass. *Sustain. Environ. Res.* 26 (3), 103–109. doi:10.1016/j.serj.2016.04.012

Huang, Y.-F., Chiueh, P.-T., and Lo, S.-L. (2019). CO2 adsorption on biochar from co-torrefaction of sewage sludge and leucaena wood using microwave heating. *Energy Procedia* 158, 4435–4440. doi:10.1016/j.egypro.2019.01.772

Isiuku, B. O., and Nwabueze, B. I. (2019). Aqueous phase Adsorption of metanil yellow on phosphoric acid-activated carbon prepared from gmelina arborea bark. *J. Chem. Soc. Niger.* 44 (1), 30–40.

Islam, M. A., Tan, I. A. W., Benhouria, A., Asif, M., and Hameed, B. H. (2015). Mesoporous and adsorptive properties of palm date seed activated carbon prepared via sequential hydrothermal carbonization and sodium hydroxide activation. *Chem. Eng. J.* 270, 187–195. doi:10.1016/j.cej.2015.01.058

Jabbar, A. (2020). Comparative study for adsorption of acidic and basic dyes on activated carbon prepared from date stone by different activation agent. *Al-Qadisiyah J. Eng. Sci.* 13, 12–20. doi:10.30772/qjes.v13i1.622

Jalandoni-Buan, A. C., Decena-Soliven, A. L. A., Cao, E. P., Barraquio, V. L., and Barraquio, W. L. (2010). Characterization and identification of Congo red decolorizing bacteria from monocultures and consortia. *Philipp. J. Sci.* 139 (1), 71–78.

Jonoobi, M., Shafie, M., Shirmohammadli, Y., Ashori, A., Hosseinabadi, H. Z., and Mekonnen, T. J. (2019). A review on date palm tree: Properties, characterization and its potential applications. *J. Renew. Mat.* 7 (11), 1055–1075. doi:10.32604/jrm.2019.08188

Kert, M., Besedič, I., and Podlipnik, Č. (2019). Influence of dye structure and temperature on the adsorption of acid dyes onto polyamide 6 knitwear. *Ind. Textila* 70 (1), 3–8. doi:10.35530/it.070.01.1400

Khadhri, N., El Khames Saad, M., ben Mosbah, M., and Moussaoui, Y. (2019). Batch and continuous column adsorption of indigo carmine onto activated carbon derived from date palm petiole. *J. Environ. Chem. Eng.* 7 (1), 102775. doi:10.1016/j.jece.2018.11.020

Khaleefa, S. A., Hamad, H. T. J. E., and Journal, T. (2019). Textile dye removal by activated date seeds. *Text. Dye Remov. by Act. Date Seeds* 37, 242–247. doi:10.30684/etj.37.2c.7

Khan, S., and Malik, A. (2018). Toxicity evaluation of textile effluents and role of native soil bacterium in biodegradation of a textile dye. *Environ. Sci. Pollut. Res.* 25 (5), 4446–4458. doi:10.1007/s11356-017-0783-7

Khan, T. A., Saud, A. S., Jamari, S. S., Rahim, M. H. A., Park, J.-W., and Kim, H.-J. (2019). Hydrothermal carbonization of lignocellulosic biomass for carbon rich material preparation: A review. *Biomass Bioenergy* 130, 105384. doi:10.1016/j.biombioe.2019.105384

Khan, T. M., Riaz, I., Hameed, S., and Khan, B. (2019). Lemon juice and microwave assisted modification of date seed husk for arsenic biosorption. *J. Innovative Sci.* 5 (2), 106–114. doi:10.17582/journal.jis/2019/5.2.106.114

Khatri, M., Ahmed, F., Shaikh, I., Phan, D.-N., Khan, Q., Khatri, Z., et al. (2017). Dyeing and characterization of regenerated cellulose nanofibers with vat dyes. *Carbohydr. Polym.* 174, 443–449. doi:10.1016/j.carbpol.2017.06.125

Knez, Ž., Markočič, E., Hrnčič, M. K., Ravber, M., and Škerget, M. J. T. (2015). High pressure water reforming of biomass for energy and chemicals: A short review. *J. Supercrit. Fluids* 96, 46–52. doi:10.1016/j.supflu.2014.06.008

Kolawole, S. A., Tijjani-Garba, H., and Omoniyi, A. O. (2022). Adsorption behaviour of methylene blue dye on eggshell extracted chitosan and carbonized date-pits as adsorbents. *J. Chem. Soc. Niger.* 47 (2), 272–283. doi:10.46602/jcsn.v47i2.725

Kozyatnyk, I., Oesterle, P., Wurzer, C., Mašek, O., and Jansson, S. (2021). Removal of contaminants of emerging concern from multicomponent systems using carbon dioxide activated biochar from lignocellulosic feedstocks. *Bioresour. Technol.* 340, 125561. doi:10.1016/j.biortech.2021.125561

Krishna Moorthy, A., Govindarajan Rathi, B., Shukla, S. P., Kumar, K., and Shree Bharti, V. (2021). Acute toxicity of textile dye Methylene blue on growth and metabolism of selected freshwater microalgae. *Environ. Toxicol. Pharmacol.* 82, 103552. doi:10.1016/j.etap.2020.103552

Kristianto, H., Susanti, R., Arie, A., Ondy, F., Chrismanto, C., and Devianto, H. (2020). Synthesis of activated carbon from Salacca peel using hydrothermal carbonization and microwave assisted chemical activation as promising supercapacitor's electrode. *AIP Conf. Proc.* 2255 (1), 060025. doi:10.1063/5.0013599

Kruse, A. (2008). Supercritical water gasification. *Biofuel. Bioprod. Biorefin.* 2 (5), 415–437. doi:10.1002/bbb.93

Kua, H. W., Pedapati, C., Lee, R. V., and Kawi, S. (2019). Effect of indoor contamination on carbon dioxide adsorption of wood-based biochar – lessons for direct air capture. *J. Clean. Prod.* 210, 860–871. doi:10.1016/j.jclepro.2018.10.206

La, H., Hettiaratchi, J. P. A., and Achari, G. (2019). The influence of biochar and compost mixtures, water content, and gas flow rate, on the continuous adsorption of methane in a fixed bed column. *J. Environ. Manag.* 233, 175–183. doi:10.1016/j.jenvman.2018.12.015

Lafta, A., Halbus, A., Athab, Z., and Hussein, F. (2014). Adsorption of reactive yellow dye 145 from wastewater onto Iraqi zahdy and khestawy date palm seeds activated carbons. *Asian J. Chem.* 26, S167–S172. doi:10.14233/ajchem.2014.19038

Lagergren, S., and Svenska, K. (1898). About the theory of so-called adsorption of soluble substances. *J. Water Resour. Prot.* 24, 1–39.

Langmuir, I. (1918). The adsorption of gases on plane surfaces of glass, mica and platinum. *J. Am. Chem. Soc.* 40 (9), 1361–1403. doi:10.1021/ja02242a004

Langmuir, I. (1916). The constitution and fundamental properties of solids and liquids. Part I. Solids. *J. Am. Chem. Soc.* 38 (11), 2221–2295. doi:10.1021/ja02268a002

Lewoyehu, M. (2021). Comprehensive review on synthesis and application of activated carbon from agricultural residues for the remediation of venomous pollutants in wastewater. *J. Anal. Appl. Pyrolysis* 159, 105279. doi:10.1016/j.jaap.2021.105279

Li, H.-Z., Zhang, Y.-N., Guo, J.-Z., Lv, J.-Q., Huan, W.-W., and Li, B. (2021). Preparation of hydrochar with high adsorption performance for methylene blue by co-hydrothermal carbonization of polyvinyl chloride and bamboo. *Bioresour. Technol.* 337, 125442. doi:10.1016/j.biortech.2021.125442

Li, H., Tian, L., Huang, B., Lu, J., Shi, S., Lu, Y., et al. (2020). Experimental study on coal damage subjected to microwave heating. *Rock Mech. Rock Eng.* 53 (12), 5631–5640. doi:10.1007/s00603-020-02230-z

Li, S.-Y., Teng, H.-J., Guo, J.-Z., Wang, Y.-X., and Li, B. (2021). Enhanced removal of Cr(VI) by nitrogen-doped hydrochar prepared from bamboo and ammonium chloride. *Bioresour. Technol.* 342, 126028. doi:10.1016/j.biortech.2021.126028

Li, Y., Zhang, D., Han, M., He, J., Wang, Y., Wang, K., et al. (2018). Fabrication of the phosphorus doped mesoporous carbon with superior capacitive performance by microwave irradiation under ambient atmosphere: An ultra-facile and energy-efficient method. *Appl. Surf. Sci.* 458, 119–128. doi:10.1016/j.apsusc.2018.07.089

Liang, J., Yu, Z., Chen, L., Fang, S., and Ma, X. (2019). Microwave pretreatment power and duration time effects on the catalytic pyrolysis behaviors and kinetics of water hyacinth. *Bioresour. Technol.* 286, 121369. doi:10.1016/j.biortech.2019.121369

Lin, C., Zhao, P., Ding, Y., Cui, X., Liu, F., Wang, C., et al. (2021). Hydrogen-rich gas production from hydrochar derived from hydrothermal carbonization of PVC and alkali coal. *Fuel Process. Technol.* 222, 106959. doi:10.1016/j.fuproc.2021.106959

Luo, J., Li, X., Ge, C., Müller, K., Yu, H., Deng, H., et al. (2021). Preparation of ammonium-modified cassava waste-derived biochar and its evaluation for synergistic adsorption of ternary antibiotics from aqueous solution. *J. Environ. Manag.* 298, 113530. doi:10.1016/j.jenvman.2021.113530

Lv, B.-W., Xu, H., Guo, J.-Z., Bai, L.-Q., and Li, B. (2022). Efficient adsorption of methylene blue on carboxylate-rich hydrochar prepared by one-step hydrothermal carbonization of bamboo and acrylic acid with ammonium persulphate. *J. Hazard. Mater.* 421, 126741. doi:10.1016/j.jhazmat.2021.126741

Ma, Q., Chen, W., Jin, Z., Chen, L., Zhou, Q., and Jiang, X. (2021). One-step synthesis of microporous nitrogen-doped biochar for efficient removal of CO2 and H2S. *Fuel* 289, 119932. doi:10.1016/j.fuel.2020.119932

Mahapatra, U., Chatterjee, A., Das, C., and Manna, A. K. (2021). Adsorptive removal of hexavalent chromium and methylene blue from simulated solution by activated carbon synthesized from natural rubber industry biosludge. *Environ. Technol. Innovation* 22, 101427. doi:10.1016/j.eti.2021.101427

Maleki, H., and Barani, H. (2019). "Extraction and antibacterial activity of pulicaria gnaphalodes as a natural colorant: Characterization and application on wool fibers. *Prog. Color Colorants Coat.*, 12, 145–154.

Mallaki, M., and Fatehi, R. (2014). Design of a biomass power plant for burning date palm waste to cogenerate electricity and distilled water. *Renew. Energy* 63, 286–291. doi:10.1016/j.renene.2013.09.036

Mari Selvam, S., and Paramasivan, B. (2022). Microwave assisted carbonization and activation of biochar for energy-environment nexus: A review. *Chemosphere* 286, 131631. doi:10.1016/j.chemosphere.2021.131631

Marland, S., Merchant, A., and Rowson, N. (2001). Dielectric properties of coal. *Fuel* 80 (13), 1839–1849. doi:10.1016/S0016-2361(01)00050-3

Marx, S., Venter, R. J., Louw, A., and Dewah, C. T. (2021). Upgrading of the aqueous product stream from hydrothermal liquefaction: Simultaneous removal of minerals and phenolic components using waste-derived hydrochar. *Biomass Bioenergy* 151, 106170. doi:10.1016/j.biombioe.2021.106170

Meerbergen, K., Crauwels, S., Willems, K. A., Dewil, R., Van Impe, J., Appels, L., et al. (2017). Decolorization of reactive azo dyes using a sequential chemical and activated sludge treatment. *J. Biosci. Bioeng.* 124 (6), 668–673. doi:10.1016/j.jbiosc.2017.07.005

Melliti, A., Srivastava, V., Kheriji, J., SillanpÄÄ, M., and Hamrouni, B. (2021). Date Palm Fiber as a novel precursor for porous activated carbon: Optimization, characterization and its application as Tylosin antibiotic scavenger from aqueous solution. *Surfaces Interfaces* 24, 101047. doi:10.1016/j.surfin.2021.101047

Messaoudi, N. E., Khomri, M. E., Bentahar, S., Dbik, A., Lacherai, A., and Bakiz, B. (2016). Evaluation of performance of chemically treated date stones: Application for the removal of cationic dyes from aqueous solutions. *J. Taiwan Inst. Chem. Eng.* 67, 244–253. doi:10.1016/j.jtice.2016.07.024

Mohamad, F. M. Y., Aziz, A., and Azmier Ahmad, M. (2022). Conversion of teak wood waste into microwave-irradiated activated carbon for cationic methylene blue dye removal: Optimization and batch studies. *Arabian J. Chem.* 15 (9), 104081. doi:10.1016/j.arabjc.2022.104081

Mohamed, B. A., Ellis, N., Kim, C. S., Bi, X., and Chen, W.-H. (2021). Engineered biochars from catalytic microwave pyrolysis for reducing heavy metals phytotoxicity and increasing plant growth. *Chemosphere* 271, 129808. doi:10.1016/j.chemosphere.2021.129808

Mohammed, S. A., Mabood, F., Abdlatef, W., Wadi, I., Yousif, E., and Abd Ali, A. (2018). Removal of dyes from simulated wastewater using low cost activated carbon derived from date pits. *Drink. Water Eng. Sci. Discuss.* 2018, 1–8. doi:10.5194/dwes-2018-1

Mortazavi-Derazkola, S., Salavati-Niasari, M., Amiri, O., and Abbasi, A. (2017). Fabrication and characterization of Fe3O4@SiO2@TiO2@Ho nanostructures as a novel and highly efficient photocatalyst for degradation of organic pollution. *J. Energy Chem.* 26 (1), 17–23. doi:10.1016/j.jechem.2016.10.015

Motasemi, F., and Afzal, M. T. (2013). A review on the microwave-assisted pyrolysis technique. *Renew. Sustain. Energy Rev.* 28, 317–330. doi:10.1016/j.rser.2013.08.008

Mumtaz, H., Farhan, M., Amjad, M., Riaz, F., Kazim, A. H., Sultan, M., et al. (2021). Biomass waste utilization for adsorbent preparation in CO2 capture and sustainable environment applications. *Sustain. Energy Technol. Assessments* 46, 101288. doi:10.1016/j.seta.2021.101288

Mustafa, R., and Asmatulu, E. (2020). Preparation of activated carbon using fruit, paper and clothing wastes for wastewater treatment. *J. Water Process Eng.* 35, 101239. doi:10.1016/j.jwpe.2020.101239

Nguyen, A., Fu, C.-C., and Juang, R.-S. (2016). Effective removal of sulfur dyes from water by biosorption and subsequent immobilized laccase degradation on crosslinked chitosan beads. *Chem. Eng. J.* 304, 313–324. doi:10.1016/j.cej.2016.06.102

Nizamuddin, S., Hossain, N., Qureshi, S. S., Al-Mohaimeed, A. M., Tanjung, F. A., Elshikh, M. S., et al. (2021). Experimental investigation of physicochemical, thermal, mechanical and rheological properties of polylactide/rice straw hydrochar composite. *J. Environ. Chem. Eng.* 9 (5), 106011. doi:10.1016/j.jece.2021.106011

Ogungbenro, A. E., Quang, D. V., Al-Ali, K. A., Vega, L. F., and Abu-Zahra, M. R. M. (2020). Synthesis and characterization of activated carbon from biomass date seeds for carbon dioxide adsorption. *J. Environ. Chem. Eng.* 8 (5), 104257. doi:10.1016/j.jece.2020.104257

Okajima, I., and Sako, T. (2013). Energy conversion of biomass with supercritical and subcritical water using large-scale plants. *J. Biosci. Bioeng.* 117, 1–9. doi:10.1016/j.jbiosc.2013.06.010

Olszewski, M. P., Nicolae, S. A., Arauzo, P. J., Titirici, M.-M., and Kruse, A. (2020). Wet and dry? Influence of hydrothermal carbonization on the pyrolysis of spent grains. *J. Clean. Prod.* 260, 121101. doi:10.1016/j.jclepro.2020.121101

Omoriyekomwan, J. E., Tahmasebi, A., Dou, J., Wang, R., and Yu, J. (2021). A review on the recent advances in the production of carbon nanotubes and carbon nanofibers via microwave-assisted pyrolysis of biomass. *Fuel Process. Technol.* 214, 106686. doi:10.1016/j.fuproc.2020.106686

Ortiz-Uribe, N., Salomón-Torres, R., and Krueger, R. (2019). Date palm status and perspective in Mexico. *Agriculture* 9 (3), 46. doi:10.3390/agriculture9030046

Pal, P., Achazhiyath Edathil, A., Chaurasia, L., K, R., and Banat, F. (2018). Removal of sulfide from aqueous solutions using novel alginate–iron oxide magnetic hydrogel composites. *Polym. Bull. Berl.* 75, 5455–5475. doi:10.1007/s00289-018-2338-6

Pauletto, P. S., Moreno-Pérez, J., Hernández-Hernández, L. E., Bonilla-Petriciolet, A., Dotto, G. L., and Salau, N. P. G. (2021). Novel biochar and hydrochar for the adsorption of 2-nitrophenol from aqueous solutions: An approach using the PVSDM model. *Chemosphere* 269, 128748. doi:10.1016/j.chemosphere.2020.128748

Plazinski, W., Rudzinski, W., and Plazinska, A. (2009). Theoretical models of sorption kinetics including a surface reaction mechanism: A review. *Adv. Colloid Interface Sci.* 152 (1), 2–13. doi:10.1016/j.cis.2009.07.009

Prajapati, A. K., and Mondal, M. K. (2020). Comprehensive kinetic and mass transfer modeling for methylene blue dye adsorption onto CuO nanoparticles loaded on nanoporous activated carbon prepared from waste coconut shell. *J. Mol. Liq.* 307, 112949. doi:10.1016/j.molliq.2020.112949

Qu, J., Lin, X., Liu, Z., Liu, Y., Wang, Z., Liu, S., et al. (2021). One-pot synthesis of Ca-based magnetic hydrochar derived from consecutive hydrothermal and pyrolysis processing of bamboo for high-performance scavenging of Pb(II) and tetracycline from water. *Bioresour. Technol.* 343, 126046. doi:10.1016/j.biortech.2021.126046

Qureshi, U. A., Hameed, B. H., and Ahmed, M. J. (2020). Adsorption of endocrine disrupting compounds and other emerging contaminants using lignocellulosic biomass-derived porous carbons: A review. *J. Water Process Eng.* 38, 101380. doi:10.1016/j.jwpe.2020.101380

Rambabu, K., AlYammahi, J., Bharath, G., Thanigaivelan, A., Sivarajasekar, N., and Banat, F. (2021). Nano-activated carbon derived from date palm coir waste for efficient sequestration of noxious 2, 4-dichlorophenoxyacetic acid herbicide. *Chemosphere* 282, 131103. doi:10.1016/j.chemosphere.2021.131103

Rápó, E., Posta, K., Csavdári, A., Vincze, B. É., Mara, G., Kovács, G., et al. (2020). Performance comparison of *Eichhornia crassipes* and Salvinia natans on azo-dye (Eriochrome black T) phytoremediation. *Cryst. (Basel).* 10 (7), 565. doi:10.3390/cryst10070565

Rawat, D., Sharma, R. S., Karmakar, S., Arora, L. S., and Mishra, V. (2018). Ecotoxic potential of a presumably non-toxic azo dye. *Ecotoxicol. Environ. Saf.* 148, 528–537. doi:10.1016/j.ecoenv.2017.10.049

Reddy, M. S., Nirmala, V., and Ashwini, C. J. (2017). Bengal Gram Seed Husk as an adsorbent for the removal of dye from aqueous solutions–Batch studies. *Arabian J. Chem.* 10, S2554–S2566. doi:10.1016/j.arabjc.2013.09.029

Redlich, O., and Peterson, D. L. (1959). A useful adsorption isotherm. *J. Phys. Chem.* 63 (6), 1024. doi:10.1021/j150576a611

Rezma, S., Birot, M., Hafiane, A., and Deleuze, H. (2017). Physically activated microporous carbon from a new biomass source: Date palm petioles. *Comptes Rendus Chim.* 20 (9), 881–887. doi:10.1016/j.crci.2017.05.003

Roginsky, S., and Zeldovich, Y. B. (1934). The catalytic oxidation of carbon monoxide on manganese dioxide. *Acta Phys. Chem. USSR* 1 (554), 2019.

Rossi, A. S., Faria, M. G., Pereira, M. S., and Ataíde, C. H. (2017). Kinetics of microwave heating and drying of drilling fluids and drill cuttings. *Dry. Technol.* 35 (9), 1130–1140. doi:10.1080/07373937.2016.1233425

Sait, H. H., Hussain, A., Bassyouni, M., Ali, I., Kanthasamy, R., Ayodele, B. V., et al. (2022). Anionic dye removal using a date palm seed-derived activated carbon/chitosan polymer microbead biocomposite. *Polym. (Basel)* 14 (12), 2503. doi:10.3390/polym14122503

Saquib, M., and Muneer, M. (2003). TiO2-mediated photocatalytic degradation of a triphenylmethane dye (gentian violet), in aqueous suspensions. *Dyes Pigments* 56 (1), 37–49. doi:10.1016/S0143-7208(02)00101-8

Saremi, F., Miroliaei, M. R., Shahabi Nejad, M., and Sheibani, H. (2020). Adsorption of tetracycline antibiotic from aqueous solutions onto vitamin B6-upgraded biochar derived from date palm leaves. *J. Mol. Liq.* 318, 114126. doi:10.1016/j.molliq.2020.114126

Sasi Kumar, N., Grekov, D., Pré, P., and Alappat, B. J. (2020). Microwave mode of heating in the preparation of porous carbon materials for adsorption and energy storage applications – an overview. *Renew. Sustain. Energy Rev.* 124, 109743. doi:10.1016/j.rser.2020.109743

Scheufele, F. B., da Silva, E. S., Cazula, B. B., Marins, D. S., Sequinel, R., Borba, C. E., et al. (2021). Mathematical modeling of low-pressure H2S adsorption by babassu biochar in fixed bed column. *J. Environ. Chem. Eng.* 9 (1), 105042. doi:10.1016/j.jece.2021.105042

Sevilla, M., and Fuertes, A. B. (2009). The production of carbon materials by hydrothermal carbonization of cellulose. *Carbon* 47, 2281–2289. doi:10.1016/j.carbon.2009.04.026

Shafiq, M., Alazba, A. A., and Amin, M. T. (2019). Synthesis, characterization, and application of date palm leaf waste-derived biochar to remove cadmium and hazardous cationic dyes from synthetic wastewater. *Arab. J. Geosci.* 12 (2), 63. doi:10.1007/s12517-018-4186-y

Shafiq, M., Alazba, A., and Amin, M. J. S. M. (2018). Removal of heavy metals from wastewater using date palm as a biosorbent: A comparative review. *Sains Malays.* 47 (1), 35–49. doi:10.17576/jsm-2018-4701-05

Shahabi Nejad, M., and Sheibani, H. (2022). Super-efficient removal of arsenic and mercury ions from wastewater by nanoporous biochar-supported poly 2-aminothiophenol. *J. Environ. Chem. Eng.* 10 (3), 107363. doi:10.1016/j.jece.2022.107363

Sharma, G., and Naushad, M. (2020). Adsorptive removal of noxious cadmium ions from aqueous medium using activated carbon/zirconium oxide composite: Isotherm and kinetic modelling. *J. Mol. Liq.* 310, 113025. doi:10.1016/j.molliq.2020.113025

Sharma, J., Sharma, S., and Soni, V. (2021). Classification and impact of synthetic textile dyes on aquatic flora: A review. *Regional Stud. Mar. Sci.* 45, 101802. doi:10.1016/j.rsma.2021.101802

Shen, Z. (2020). Coordinated environment and economy in coastal development based on industrial wastewater and so2 emissions. *J. Coast. Res.* 109, 13–18. doi:10.2112/JCR-SI109-003.1

Shi, Z., Usman, M., He, J., Chen, H., Zhang, S., and Luo, G. (2021). Combined microbial transcript and metabolic analysis reveals the different roles of hydrochar and biochar in promoting anaerobic digestion of waste activated sludge. *Water Res.* 205, 117679. doi:10.1016/j.watres.2021.117679

Shoaib, M., and Al-Swaidan, H. M. (2015). Optimization and characterization of sliced activated carbon prepared from date palm tree fronds by physical activation. *Biomass Bioenergy* 73, 124–134. doi:10.1016/j.biombioe.2014.12.016

Sims, R. A., Harmer, S. L., and Quinton, J. S. (2019). The role of physisorption and chemisorption in the oscillatory adsorption of organosilanes on aluminium oxide. *Polym. (Basel).* 11 (3), 410. doi:10.3390/polym11030410

Sips, R. (1948). On the structure of a catalyst surface. *J. Chem. Phys.* 16 (5), 490–495. doi:10.1063/1.1746922

Sultana, A. I., Saha, N., and Reza, M. T. (2021). Upcycling simulated food wastes into superactivated hydrochar for remarkable hydrogen storage. *J. Anal. Appl. Pyrolysis* 159, 105322. doi:10.1016/j.jaap.2021.105322

Sun, Y., Gao, B., Yao, Y., Fang, J., Zhang, M., Zhou, Y., et al. (2014). Effects of feedstock type, production method, and pyrolysis temperature on biochar and hydrochar properties. *Chem. Eng. J.* 240, 574–578. doi:10.1016/j.cej.2013.10.081

Tahir, A. H., Al-Obaidy, A. H. M., and Mohammed, F. H. (2020). Biochar from date palm waste, production, characteristics and use in the treatment of pollutants: A review. *IOP Conf. Ser. Mat. Sci. Eng.* 737, 012171. IOP Publishing. doi:10.1088/1757-899X/737/1/012171

Tan, K. L., and Hameed, B. H. (2017). Insight into the adsorption kinetics models for the removal of contaminants from aqueous solutions. *J. Taiwan Inst. Chem. Eng.* 74, 25–48. doi:10.1016/j.jtice.2017.01.024

Temkin, M., and Pyzhev, V. (1940). Kinetics of ammonia synthesis on promoted iron catalysts. *Acta Physicochim. URSS* 12, 217–222.

Varjani, S., Rakholiya, P., Ng, H. Y., You, S., and Teixeira, J. A. (2020). Microbial degradation of dyes: An overview. *Bioresour. Technol.* 314, 123728. doi:10.1016/j.biortech.2020.123728

Villota, S. M., Lei, H., Villota, E., Qian, M., Lavarias, J., Taylan, V., et al. (2019). Microwave-Assisted activation of waste cocoa pod husk by H3PO4 and KOH—comparative insight into textural properties and pore development. *ACS Omega* 4 (4), 7088–7095. doi:10.1021/acsomega.8b03514

Wang, T., Wu, J., Zhang, Y., Liu, J., Sui, Z., Zhang, H., et al. (2018). Increasing the chlorine active sites in the micropores of biochar for improved mercury adsorption. *Fuel* 229, 60–67. doi:10.1016/j.fuel.2018.05.028

Weber, W. J., and Morris, J. C. (1963). Kinetics of adsorption on carbon from solution. *J. Sanit. Engrg. Div.* 89 (2), 31–59. doi:10.1061/jsedai.0000430

Yadav, S., Asthana, A., Singh, A. K., Chakraborty, R., Vidya, S. S., Susan, M. A. B. H., et al. (2021). Adsorption of cationic dyes, drugs and metal from aqueous solutions using a polymer composite of magnetic/β-cyclodextrin/activated charcoal/Na alginate: Isotherm, kinetics and regeneration studies. *J. Hazard. Mater.* 409, 124840. doi:10.1016/j.jhazmat.2020.124840

Yamil, L. d. O., Georgin, J., Franco, D. S., Netto, M. S., Piccilli, D. G., Foletto, E. L., et al. (2021). High-performance removal of 2, 4-dichlorophenoxyacetic acid herbicide in water using activated carbon derived from Queen palm fruit endocarp. *Syagrus romanzoffiana)* 9 (1), 104911.

Yan, H., Niu, Q., Zhu, Q., Wang, S., Meng, Q., Li, G., et al. (2021). Biochar reinforced the populations of cbbL-containing autotrophic microbes and humic substance formation via sequestrating CO2 in composting process. *J. Biotechnol.* 333, 39–48. doi:10.1016/j.jbiotec.2021.04.011

Yan, X.-F., Fan, X.-R., Wang, Q., and Shen, Y. J. T. S. (2017). An adsorption isotherm model for adsorption performance of silver-loaded activated carbon. *Therm. Sci.* 21 (4), 1645–1649. doi:10.2298/tsci151202048y

Yang, Z., Shen, W., Chen, Q., and Wang, W. (2021). Direct electrochemical reduction and dyeing properties of CI Vat Yellow 1 using carbon felt electrode. *Dyes Pigments* 184, 108835. doi:10.1016/j.dyepig.2020.108835

Yu, C., Shao, Y., Wang, K., and Zhang, L. (2019). A group decision making sustainable supplier selection approach using extended TOPSIS under interval-valued Pythagorean fuzzy environment. *Expert Syst. Appl.* 121, 1–17. doi:10.1016/j.eswa.2018.12.010

Yuan, Y., Huang, L., Zhang, T. C., Ouyang, L., and Yuan, S. (2021). One-step synthesis of ZnFe2O4-loaded biochar derived from leftover rice for high-performance H2S removal. *Sep. Purif. Technol.* 279, 119686. doi:10.1016/j.seppur.2021.119686

Yusop, M. F. M., Ahmad, M. A., Rosli, N. A., Gonawan, F. N., and Abdullah, S. J. (2021a). Scavenging malachite green dye from aqueous solution using durian peel based activated carbon. *Mal. J. Fund. Appl. Sci.* 17 (1), 95–103. doi:10.11113/mjfas.v17n1.2173

Yusop, M. F. M., Ahmad, M. A., Rosli, N. A., and Manaf, M. E. A. (2021b). Adsorption of cationic methylene blue dye using microwave-assisted activated carbon derived from acacia wood: Optimization and batch studies. *Arabian J. Chem.* 14 (6), 103122. doi:10.1016/j.arabjc.2021.103122

Yusop, M. F. M., Jaya, E. M. J., and Ahmad, M. A. (2022a). Single-stage microwave assisted coconut shell based activated carbon for removal of Zn(II) ions from aqueous solution – optimization and batch studies. *Arabian J. Chem.* 15 (8), 104011. doi:10.1016/j.arabjc.2022.104011

Yusop, M. F. M., Jaya, E. M. J., Din, A. T. M., Bello, O. S., and Ahmad, M. A. (2022b). Single-stage optimized microwave-induced activated carbon from coconut shell for cadmium adsorption. *Chem. Eng. Technol.* doi:10.1002/ceat.202200051

Zama, E. F., Zhu, Y.-G., Reid, B. J., and Sun, G.-X. (2017). The role of biochar properties in influencing the sorption and desorption of Pb(II), Cd(II) and As(III) in aqueous solution. *J. Clean. Prod.* 148, 127–136. doi:10.1016/j.jclepro.2017.01.125

Zarei, M., Mohammadzadeh, I., Saidi, K., and Sheibani, H. (2022). Fabrication of biochar@Cu-Ni nanocatalyst for reduction of aryl aldehyde and nitroarene compounds. *Biomass Convers. biorefin.* doi:10.1007/s13399-022-02490-5

Zarei, M., Seyedi, N., Maghsoudi, S., Nejad, M. S., and Sheibani, H. (2021). Green synthesis of Ag nanoparticles on the modified graphene oxide using Capparis spinosa fruit extract for catalytic reduction of organic dyes. *Inorg. Chem. Commun.* 123, 108327. doi:10.1016/j.inoche.2020.108327

Zhang, J., Shao, J., Huang, D., Feng, Y., Zhang, X., Zhang, S., et al. (2020). Influence of different precursors on the characteristic of nitrogen-enriched biochar and SO2 adsorption properties. *Chem. Eng. J.* 385, 123932. doi:10.1016/j.cej.2019.123932

Zhang, J., Wang, Y., Wang, X., Wu, W., Cui, X., Cheng, Z., et al. (2022). Hydrothermal conversion of Cd/Zn hyperaccumulator (Sedum alfredii) for heavy metal separation and hydrochar production. *J. Hazard. Mater.* 423, 127122. doi:10.1016/j.jhazmat.2021.127122

Zhang, X., Zhang, S., Yang, H., Shao, J., Chen, Y., Feng, Y., et al. (2015). Effects of hydrofluoric acid pre-deashing of rice husk on physicochemical properties and CO2 adsorption performance of nitrogen-enriched biochar. *Energy* 91, 903–910. doi:10.1016/j.energy.2015.08.028

Zhang, X., Zheng, H., Li, G., Gu, J., Shao, J., Zhang, S., et al. (2021). Ammoniated and activated microporous biochar for enhancement of SO2 adsorption. *J. Anal. Appl. Pyrolysis* 156, 105119. doi:10.1016/j.jaap.2021.105119

Zhang, Z., Yang, J., Qian, J., Zhao, Y., Wang, T., and Zhai, Y. (2021). Biowaste hydrothermal carbonization for hydrochar valorization: Skeleton structure, conversion pathways and clean biofuel applications. *Bioresour. Technol.* 324, 124686. doi:10.1016/j.biortech.2021.124686

Zhou, S., Du, Z., Li, X., Zhang, Y., He, Y., and Zhang, Y. (2019). Degradation of methylene blue by natural manganese oxides: Kinetics and transformation products. *R. Soc. open Sci.* 6 (7), 190351. doi:10.1098/rsos.190351

Zhu, J., Song, Y., Wang, L., Zhang, Z., Gao, J., Tsang, D. C. W., et al. (2021). Green remediation of benzene contaminated groundwater using persulfate activated by biochar composite loaded with iron sulfide minerals. *Chem. Eng. J.* 429, 132292. doi:10.1016/j.cej.2021.132292

Zhu, Y., Yi, B., Yuan, Q., Wu, Y., Wang, M., and Yan, S. (2018). Removal of methylene blue from aqueous solution by cattle manure-derived low temperature biochar. *RSC Adv.* 8 (36), 19917–19929. doi:10.1039/C8RA03018A

Zlotorzynski, A. (1995). The application of microwave radiation to analytical and environmental chemistry. *Crit. Rev. Anal. Chem.* 25 (1), 43–76. doi:10.1080/10408349508050557

Zubair, M., Manzar, M. S., Mu'azu, N. D., Anil, I., Blaisi, N. I., and Al-Harthi, M. A. (2020a). Functionalized MgAl-layered hydroxide intercalated date-palm biochar for Enhanced Uptake of Cationic dye: Kinetics, isotherm and thermodynamic studies. *Appl. Clay Sci.* 190, 105587. doi:10.1016/j.clay.2020.105587

Zubair, M., Mu'azu, N. D., Jarrah, N., Blaisi, N. I., Aziz, H. A., and Al-Harthi, M. (2020b). Adsorption behavior and mechanism of methylene blue, crystal violet, Eriochrome black T, and methyl orange dyes onto biochar-derived date palm fronds waste produced at different pyrolysis conditions. *Water Air Soil Pollut.* 231 (5), 240. doi:10.1007/s11270-020-04595-x